Available online at www.sciencedirect.com
ScienceDirect
Geochimica et Cosmochimica Acta 73 (2009) 6187–6204
Geochimica et Cosmochimica Acta
www.elsevier.com/locate/gca

The effect of sulfate concentration on (sub)millimeter-scale sulfide $\delta^{34}S$ in hypersaline cyanobacterial mats over the diurnal cycle

David A. Fike [a,b,*], Niko Finke [c,d], Jessica Zha [e], Garrett Blake [f], Tori M. Hoehler [c], Victoria J. Orphan [a,*]

[a] *Division of Geological & Planetary Sciences, California Institute of Technology, Pasadena, CA 91125, United States*
[b] *Department of Earth & Planetary Sciences & McDonnell Center for the Space Sciences, Washington University, St. Louis, MO 63130, United States*
[c] *NASA Ames Research Center, Moffett Field, CA 94035, United States*
[d] *Nordic Center for Earth Evolution, University of Southern Denmark, 5230 Odense M, Denmark*
[e] *Johns Hopkins University, Baltimore, MD 21218, United States*
[f] *Pitzer College, Claremont, CA 91711, United States*

Received 9 January 2009; accepted in revised form 6 July 2009; available online 12 July 2009

Abstract

Substantial isotopic fractionations are associated with many microbial sulfur metabolisms and measurements of the bulk $\delta^{34}S$ isotopic composition of sulfur species (predominantly sulfates and/or sulfides) have been a key component in developing our understanding of both modern and ancient biogeochemical cycling. However, the interpretations of bulk $\delta^{34}S$ measurements are often non-unique, making reconstructions of paleoenvironmental conditions or microbial ecology challenging. In particular, the link between the μm-scale microbial activity that generates isotopic signatures and their eventual preservation as a bulk rock value in the geologic record has remained elusive, in large part because of the difficulty of extracting sufficient material at small scales. Here we investigate the potential for small-scale (~100 μm–1 cm) $\delta^{34}S$ variability to provide additional constraints for environmental and/or ecological reconstructions. We have investigated the impact of sulfate concentrations (0.2, 1, and 80 mM SO_4) on the $\delta^{34}S$ composition of hydrogen sulfide produced over the diurnal (day/night) cycle in cyanobacterial mats from Guerrero Negro, Baja California Sur, Mexico. Sulfide was captured as silver sulfide on the surface of a 2.5 cm metallic silver disk partially submerged beneath the mat surface. Subsequent analyses were conducted on a Cameca 7f-GEO secondary ion mass spectrometer (SIMS) to record spatial $\delta^{34}S$ variability within the mats under different environmental conditions. Isotope measurements were made in a 2-dimensional grid for each incubation, documenting both lateral and vertical isotopic variation within the mats. Typical grids consisted of ~400–800 individual measurements covering a lateral distance of ~1 mm and a vertical depth of ~5–15 mm. There is a large isotopic enrichment (~10–20‰) in the uppermost mm of sulfide in those mats where $[SO_4]$ was non-limiting (field and lab incubations at 80 mM). This is attributed to rapid recycling of sulfur (elevated sulfate reduction rates and extensive sulfide oxidation) at and above the chemocline. This isotopic gradient is observed in both day and night enrichments and suggests that, despite the close physical association between cyanobacteria and select sulfate-reducing bacteria, photosynthetic forcing has no substantive impact on $\delta^{34}S$ in these cyanobacterial mats. Perhaps equally surprising, large, spatially-coherent $\delta^{34}S$ oscillations (~20–30‰ over 1 mm) occurred at depths up to ~1.5 cm below the mat surface. These gradients must arise *in situ* from differential microbial metabolic activity and fractionation during sulfide production at depth. Sulfate concentrations were the dominant control on the spatial variability of sulfide $\delta^{34}S$. Decreased sulfate concentrations diminished both vertical and lateral $\delta^{34}S$ variability, suggesting that small-scale variations of $\delta^{34}S$ can be diagnostic for reconstructing past sulfate concentrations, even when original sulfate $\delta^{34}S$ is unknown.

* Corresponding authors. Tel.: +1 314 935 6607 (D.A. Fike), +1 626 395 1786 (V.J. Orphan).
E-mail addresses: dfike@levee.wustl.edu (D.A. Fike), vorphan@gps.caltech.edu (V.J. Orphan).

0016-7037/$ - see front matter © 2009 Elsevier Ltd. All rights reserved.
doi:10.1016/j.gca.2009.07.006

1. INTRODUCTION

The sulfur cycle is one of the principal biogeochemical regulators of Earth's surface redox over geologic time (Garrels and Lerman, 1981; Holser et al., 1988; Berner, 2006). Measurements of the sulfur isotopic composition ($\delta^{34}S_x = ((^{34}S/^{32}S)_x/(^{34}S/^{32}S)_{STD} - 1)*10^3$, reported in permil (‰) relative to the international V-CDT standard) of sulfate and sulfide minerals have been instrumental for reconstructing modern and ancient sulfur cycling (Thode and Monster, 1965; Holser and Kaplan, 1966; Holser, 1977; Claypool et al., 1980; Thode, 1980; Ross et al., 1995; Canfield and Teske, 1996; Hurtgen et al., 2004, 2005; Kampschulte and Strauss, 2004; Gill et al., 2007; Fike et al., 2006; Fike and Grotzinger, 2008). The fractionation between coeval sulfate and sulfide phases results primarily from microbial metabolic activity and thus encodes information about the dominant microbial metabolisms and prevailing geochemical conditions (Fry et al., 1984, 1985, 1986a; Canfield and Des Marais, 1993; Canfield and Thamdrup, 1994; Canfield and Teske, 1996; Habicht and Canfield, 1996, 1997; Canfield et al., 1998; Habicht et al., 1998, 2002; Canfield, 2001a; Detmers et al., 2001).

The type and relative activity of different microbial sulfur metabolisms (e.g., reduction, disproportionation, oxidation) place first-order controls on sulfur isotope fractionations (Harrison and Thode, 1958; Kaplan and Rittenberg, 1964; Kemp and Thode, 1968; Rees, 1973; Fry et al., 1984, 1985; Canfield and Thamdrup, 1994; Canfield and Teske, 1996; Canfield et al., 1998; Habicht et al., 1998). The fractionation during bacterial sulfate reduction (BSR) is thought to be the main driver of sulfate and sulfide $\delta^{34}S$ in the geologic record (Canfield, 2001a; Habicht et al., 2002). Additional metabolisms, particularly sulfur disproportionation (Bak and Cypionka, 1987; Jorgensen, 1990, 1994; Fuseler and Cypionka, 1995; Cypionka et al., 1998; Finster et al., 1998), are capable of adding additional fractionations (Canfield and Thamdrup, 1994; Canfield et al., 1998; Habicht et al., 1998). Based on the magnitude of coeval sulfate–sulfide fractionation, the environmental importance of these auxiliary metabolisms is believed to have increased in the last ~580 million years, as the oxidative sulfur cycle began to play an increasingly important role (Canfield and Teske, 1996; Hurtgen et al., 2005; Fike et al., 2006).

Fractionation during BSR itself is highly variable and depends upon a variety of biological and environmental parameters (Fig. 1). The most relevant parameters controlling fractionation during BSR include sulfate concentration, sulfate reduction rate, electron donor, and temperature (Harrison and Thode, 1958; Kaplan and Rittenberg, 1964; Chambers et al., 1975; Canfield, 2001a,b; Habicht et al., 2002). The effect of sulfate concentration on isotopic fractionation is fairly well understood from both theoretical and experimental work (Harrison and Thode, 1958; Canfield, 2001b; Habicht et al., 2002): sulfate concentrations below ~200 μM preclude significant fractionation, whereas higher concentrations (up to modern seawater) are generally correlated with increasing fractionation to ca. 30‰. Elevated sulfate reduction rates are typically associated with decreased fractionation, especially for organic electron donors (Kaplan and Rittenberg, 1964; Chambers et al., 1975; Canfield, 2001a), although this trend is not universal (Canfield et al., 2006). Isotopic fractionation with hydrogen as an electron donor generally results in smaller fractionations than with an organic electron donor, and with less dependence on sulfate reduction rates (Canfield, 2001a). Fractionations are often maximal when organisms are at their optimal growth temperature (Canfield, 2001a); however, the complex relationships between temperature, microbial growth, and metabolic activity mean that the temperature–fractionation relationship is variable (Canfield et al., 2006).

Because multiple environmental, metabolic, and ecological factors influence the fractionation between sulfate and coexisting sulfide (Fry et al., 1986a, 1988a; Habicht and Canfield, 1997; Habicht et al., 1998; Canfield, 2001a; Wortmann et al., 2001; Werne et al., 2003; Canfield et al., 2006), reconstructions of sulfur cycling (both modern and ancient) based on bulk $\delta^{34}S$ values are commonly non-unique. One approach to placing additional constraints on sulfur cycling can be provided by analyzing small deviations from traditional mass-dependent relationships in minor sulfur isotopes ($\Delta^{33}S$, $\Delta^{36}S$) that are attributed to different microbial metabolic pathways (Farquhar et al., 2003; Johnston et al., 2005) [but see (Watanabe et al., 2009)]. Here, we advocate a different approach, focusing instead on the information encoded in the spatial variability of $\delta^{34}S$ on the ~100 μm–cm scale. Measurements of variability on these finer spatial scales, more relevant to microbial activity, are likely to encode additional information beyond that contained in bulk isotope measurements.

Previous work using a similar approach to that presented here highlighted significant (>30‰) isotopic variability at the μm- to mm-scale found within modern microbial mats (Fike et al., 2008). It is our aim in the present paper to further constrain the causes for this and other small-scale isotopic variability by investigating the impact of specific environmental conditions on observed fine-scale (100 μm–1 cm) $\delta^{34}S$ patterns. Specifically, we investigate the impact of varying sulfate concentrations and of diurnal redox forcing from photosynthesis on the absolute value and spatial variability of sulfide $\delta^{34}S$ within modern microbial mats. A refined understanding of how these parameters are linked to $\delta^{34}S$ will improve our ability both to understand modern biogeochemical cycling and to interpret the biological significance of geochemical patterns in the rock record.

2. FIELD SITE AND EXISTING CONTEXT

We analyzed microbial mats from the Exportadora del Sal, S.A. salt works, Guerrero Negro, Baja California Sur, Mexico. This system has been well characterized for its bulk microbiological community structure (Risatti et al., 1994; Spear et al., 2003; Ley et al., 2006; Green et al., 2008; Jahnke et al., 2008; Kunin et al., 2008; Orphan et al., 2008; Robertson et al., 2009), large-scale sulfur cycling (Canfield and Des Marais, 1993; Jorgensen, 1994), and the diurnal variations that arise from photosynthetic redox changes (Canfield and Des Marais, 1993; Jorgensen,

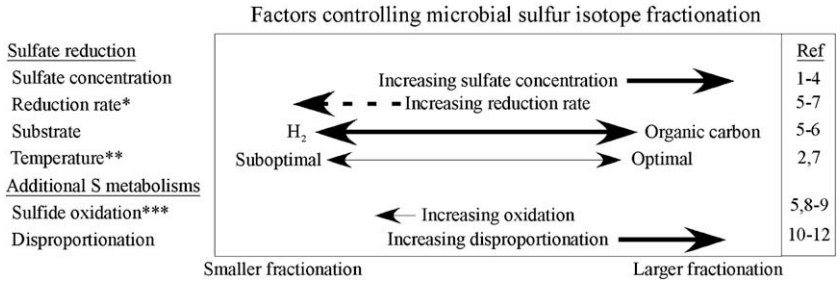

Fig. 1. Controls on sulfur isotope fractionation during microbial sulfur cycling. Thick arrows indicate trends that are well supported by the data; thin arrows reflect relationships that are less clear or direct. *Dashed line indicates that while changing sulfate reduction rates has a strong impact on fractionation during BSR with an organic electron donor, it has little effect when H_2 is the electron donor. **Temperature impacts many other microbial growth and metabolic factors and in ecologically-diverse environmental samples, the relationship with fractionation is not straightforward. ***The fractionation(s) during biological sulfide oxidation remain poorly constrained and merit additional study. References are: (1) (Harrison and Thode, 1958); (2) (Canfield et al., 2000); (3) (Canfield, 2001b); (4) (Habicht et al., 2002); (5) (Kaplan and Rittenberg, 1964); (6) (Chambers et al., 1975); (7) (Canfield et al., 2006); (8) (Fry et al., 1984); (9) (Fry et al., 1986a); (10) (Canfield and Thamdrup, 1994); (11) (Canfield et al., 1998); (12) (Habicht et al., 1998).

1994; Visscher et al., 2003; Decker et al., 2005). These *Microcoleus*-dominated mats support active aerotolerant sulfate reducers (Teske et al., 1998) in the photosynthetically-active uppermost few mm as well as anerobic sulfate reduction in the permanently anoxic zones beneath the chemocline (Canfield and Des Marais, 1993). Existing data point to a complex architecture governing the distribution of sulfate-reducing microorganisms with depth within the Guerrero Negro mats and similar mat environments (Risatti et al., 1994; Minz et al., 1999a; Fike et al., 2008; Fourcans et al., 2008).

Field sampling was done in a hypersaline pond (salinity of 90 ppt (g/kg)) known as pond 4 near 5 (P4n5). A detailed description of the area and mat geochemistry is provided in Des Marais et al. (1989) and Hoehler et al. (2001). P4n5 mats are permanently submerged in approximately 1 m of pond water with a seasonal *in situ* temperature ranging from 14 to 29 °C. P4n5 is situated on top of a gypsum pan and characterized by high levels of sulfate (80 mM) throughout the mat and in the overlying water. Such high sulfate concentrations are ideal for studying isotopic variations associated with sulfide production because the natural levels of sulfide produced (~500 μM) are insufficient to appreciably alter the original sulfate $\delta^{34}S$ composition: under these conditions mass balance limits localized variation in $\delta^{34}S$ due to enhanced sulfide oxidation or sulfate reduction to less than 0.2‰. This is not the case for experimental greenhouse incubations maintained at lower SO_4 concentrations (1 and 0.2 mM SO_4), where sulfide concentrations can be an appreciable fraction of initial sulfate concentrations (see below).

2.1. NASA Ames greenhouse facility

Sections of the subtidal mats from P4n5 measuring ~20 cm × 25 cm were collected in triplicate from Guerrero Negro in March 2006 (Fig. 2a). The mat sections were maintained in flumes under normal sunlight conditions at the dedicated greenhouse facility at NASA Ames Research Center in Moffett Field, CA as described in Bebout et al. (2002). The individual mat sections were maintained at different sulfate concentrations (80 mM (environmental levels), 1 mM, and 0.2 mM SO_4) prior to sampling in August 2007. The sulfate concentrations in the 80 mM mat were held fixed over the 17 months in which they remained in the Ames Greenhouse. Sulfate concentrations in the 1 mM mat were decreased from environmental levels to 1 mM over 7 months and then held at 1 mM from October 2006 until they were sampled in August 2007. Sulfate concentrations in the 0.2 mM mat were decreased from environmental levels to 0.2 mM over 1 year and then held at 0.2 mM from March 2007 until they were sampled in August 2007. Rapid recycling of sulfate within the mats precluded attempts to lower sulfate concentration beyond 0.2 mM (Bebout et al., 2004). This 17-month interval between mat collection and our silver disk incubations allowed the microbial community to equilibrate to the new geochemical environment – in particular, the experimental sulfate concentrations for the different incubations and the isotopic composition of the sulfate used in the experiments, which at -0.7 ± 0.1‰ is offset from the Guerrero Negro value of 21.0 ± 0.1‰.

3. ANALYTICAL PROCEDURES

3.1. Incubations

Sulfide was captured from the microbial mats by precipitation onto a 2.5 cm silver disk (Fike et al., 2008), inspired by earlier ^{35}S radioisotope experiments designed to generate two-dimensional maps of sulfate reduction (Cohen, 1984; Cohen and Helman, 1997; Visscher et al., 2000). Silver disks were polished with 1 μm colloidal alumina paste (Buehler; Lake Bluff, IL, USA) and allowed to form an oxidized surface coating under exposure to atmospheric oxygen prior to deployment. Previous comparisons between microelectrode generated sulfide profiles and the silver disk incubations has shown that the amount of sulfide that templates on the disk is generally proportional to the ambient sulfide concentration (Fike et al., 2008). As these incubations occur over a fixed time interval, however, other factors may play an important role in modifying the sulfide signal. In particular,

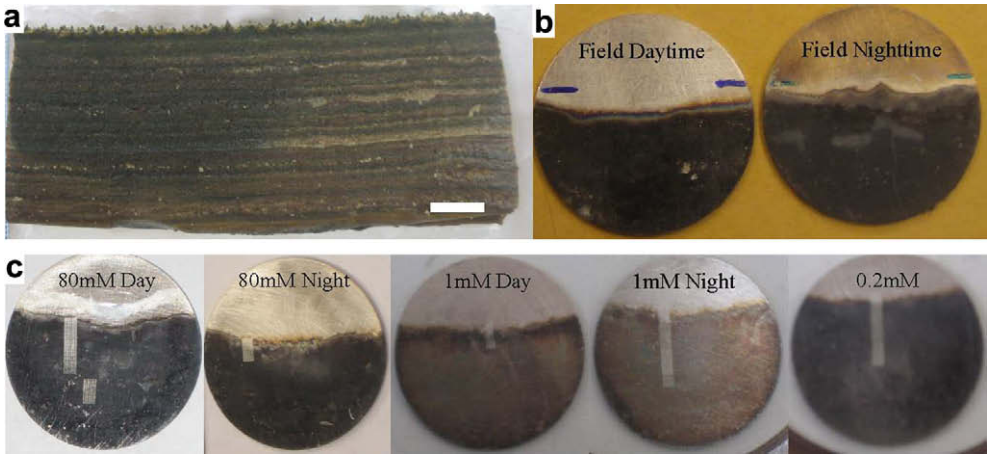

Fig. 2. Subtidal hypersaline *Microcoleus*-dominated microbial mats from Guerrero Negro. (a) Example of subtidal mats (scale bar 1 cm). (b) Day and night incubations from the field. Mat surfaces are indicated in marker at the sides of the disks. Sulfide deposition occurs ~2.7 mm below the mat surface during the day and contours the irregular surface of the mat at night. Note there is some sulfide captured from the water column during the night incubation. (c) Incubations on mats maintained at the NASA Ames Research Center greenhouse facility. 80 and 1 mM incubations were done during the day and night, while the 0.2 mM incubation was done for 24 h. See Table 1 for list of all disks examined.

high sulfate reduction rates (SRR) will cause proportionally higher amounts of sulfide to template out on the disk compared to depths with lower SRR for the same ambient sulfide concentration (e.g., 1 mM incubations in Fig. 2). Biological sulfide oxidation may also compete for sulfide and limit precipitation on the disk. Similarly, differential diffusivity of different layers of the mat (Wieland et al., 2001) will influence the amount of sulfide from adjacent regions that can reach the disk (experiments to evaluate the isotopic impact of diffusion are discussed below). As such, sulfide concentrations on the disk cannot (and should not) be directly correlated to ambient sulfide concentration. To this end, sulfide yields are reported as normalized values (0–1, with 1 as the maximum sulfide yield for that incubation). Nonetheless, they record qualitative information about relative sulfide levels and comparative rates of sulfate reduction. Because these incubations occur over many hours, whatever high frequency time variations exist within the mats are smoothed over to some extent (both in terms of the amount of sulfide templating onto the disk and its isotopic composition). As such, it is likely that the spatial variations measured by SIMS represent minimum estimates for actual *in situ* variability. However, broad trends in $\delta^{34}S$ can be examined between the day and nighttime incubations.

Disks were inserted vertically into the microbial mats, typically leaving approximately 0.5 cm of the disk exposed in the overlying water. The mat–water surface was marked onto the silver disk during incubation and subsequently indicated with permanent marker (Fig. 2b). This method of sulfide capture preserves fine-scale spatial variability within microbial systems (Visscher et al., 2000; Fike et al., 2008). Field incubations were done in the hypersaline (80 mM SO_4) subtidal mats at Guerrero Negro during the day and the night (Fig. 2b). Day and night incubations were also done at the NASA Ames greenhouse facility high (80 mM SO_4) and medium (1 mM SO_4) sulfate incubations (Fig. 2c). These incubations were all conducted over a ~12 h time period (ca. 6 AM to 6 PM 'day' and 6 PM to 6 AM 'night'). An additional incubation in the low sulfate (0.2 mM) mat at the NASA Ames greenhouse facility was done over ~24 h in order for sufficient sulfide to template onto the disk (Fig. 2c). Table 1 contains a list of these incubations as well as control experiments to evaluate the effects of diffusion and abiotic sulfide oxidation (see below). For the incubations at NASA Ames, the incubations in all three sulfate systems (80, 1, 0.2 mM) were conducted in parallel with microelectrode measurements and other geochemical and microbiological sampling. Images of the incubated disks are shown in Fig. 2 (note some images depict the disks after SIMS analysis).

3.2. Diffusion and oxidation experiments

A series of abiotic experiments were conducted to assess the impact of diffusion, abiotic oxidation, and pH on the sulfide $\delta^{34}S$ signal from our microbial mat incubations. All experiments involved a block of 1% agar (approximately 2 cm thick) containing 5 mM Na_2S buffered at either pH 7 or pH 8. To evaluate the impact of diffusion and abiotic oxidation on $\delta^{34}S$ profiles, these experiments were conducted either in an anaerobic chamber under N_2-purged water ('anaerobic' treatment) or alternatively incubated on the bench and overlain by oxygenated water ('oxic stagnant' treatment). An additional oxic treatment consisted of a sulfidic agar plug overlain with water that was actively oxygenated by bubbling air through it ('oxic agitated' treatment). For each treatment, the water and sulfidic agar were allowed to equilibrate for several hours prior to sulfide capture. To capture sulfide, a strip of photographic film (Ilford 100 Delta Professional B&W, Ilford, Cheshire, UK) was inserted into the agar and incubated for 1 h, allowing for sulfide within the agar and overlying water to react with the silver emulsion in the film. Initial experiments showed that

Table 1
Silver disk incubations for sulfide capture in microbial mats and agar.

Location[a]	Sample type	Sulfate (mM)	Period[b]
Guerrero Negro, P4n5	Subtidal mat	80	Day
Guerrero Negro, P4n5	Subtidal mat	80	Night
Greenhouse, flume 1	Subtidal mat	80	Day
Greenhouse, flume 1	Subtidal mat	80	Night
Greenhouse, flume 2	Subtidal mat	1	Day
Greenhouse, flume 2	Subtidal mat	1	Night
Greenhouse, flume 3	Subtidal mat	0.2	24 h
Lab (oxic, stagnant)	Agar[c], pH 7	–	1 h
Lab (oxic, stagnant)	Agar[c], pH 8	–	1 h
Lab (oxic, agitated)	Agar[c], pH 7	–	1 h
Lab (oxic, agitated)	Agar[c], pH 8	–	1 h
Lab (anaerobic)	Agar[c], pH 7	–	1 h
Lab (anaerobic)	Agar[c], pH 8	–	1 h

[a] See text for detailed description of laboratory agar experiments.
[b] Day incubation from ~6 AM to ~6 PM; night incubation from ~6 PM to ~6 AM.
[c] Sulfide concentration in agar (5 mM).

the sulfide templated onto silver-containing photographic film and onto silver disks gave comparable results under SIMS analysis (data not shown).

3.3. SIMS analysis and calibration

Disks were analyzed over a 10-month period (Feb–Nov 2008) on a Cameca 7f-GEO magnetic sector secondary ion mass spectrometer (SIMS) at the Caltech Center for Microanalysis. Analyses were conducted with a primary beam current of ~5 nA, corresponding to a primary beam size of ~10 μm. The primary beam was rastered over an area of 25 μm by 25 μm, with individual measurements taking approximately 4 min. Ions were collected using Faraday cups with ^{32}S collected on FC1 and ^{34}S collected on FC2. At this current, typical secondary ion yields were: ^{32}S $\sim 2*10^8$ counts/s; ^{34}S $\sim 10^7$ counts/s. For reference, Faraday cup background levels were FC1 $\sim 5*10^4$ counts/s and FC2 $\sim 3*10^3$ counts/s. Backgrounds and ion yields on the Faraday cups were recalibrated daily. Automatic peak centering (field and contrast apertures) and mass calibration occurred at the start of each measurement to correct for any drift in the magnetic field or position of the secondary ion beam. No pre-sputtering occurred beyond that during this calibration process.

Each measurement was divided into 20 cycles, where each cycle consisted of collection of ^{32}S for 1s on FC1 and collection of ^{34}S for 5s on FC2. The individual cycles were screened for anomalous points (e.g., those arising from electronic errors). An isotope cycle was considered anomalous if it was more than 3.5σ away from the average $\delta^{34}S$ value of the 20 cycles. Average isotopic compositions and standard deviations were recalculated excluding any anomalous cycles. Approximately 1% of the measurements had an anomalous cycle. The correction of these points had no substantive effect on isotopic trends in our disk incubations, but decreased the standard error associated with these particular measurements. The internal error (standard error of $n = 20$ cycles) of individual measurements was typically ~1‰ (Fig. 3). The external error (standard deviation of multiple adjacent points on standards) was ~1‰. Both values are substantially smaller than the up to 50‰ variation observed within our samples. Error generally scaled with the concentration of sulfide in the sample (i.e., error was counting-statistics limited): samples analyzed from the zone of minimal sulfide near the mat surface therefore had larger errors than those at depth. The ionization of the sulfide layers during analysis precluded establishing a steady-state ion yield (Fike et al., 2008) and ultimately limits the precision of these analyses.

Instrumental mass fractionation (IMF) was corrected for by standard-sample bracketing. Previous work examining a variety of sulfide standards suggested that a sodium sulfide solution (Na_2S) of known isotopic composition (−0.2‰) precipitated onto a silver disk was the most appropriate standard (Fike et al., 2008). The average isotopic composition of replicate analyses of this sulfide standard on the SIMS was -27.2 ± 1.0‰ (1σ standard deviation), resulting in typical IMF for these sulfide measurements of 27.0‰. This mass fractionation varied depending on instrument conditions, but the isotopic offset between standards and a given sample was independent of instrument conditions.

We assessed the impact of instrument drift on $\delta^{34}S$ over the course of our measurements by two methods. First, we observed the drift in $\delta^{34}S$ composition of known standards at the beginning and end of a sequence of samples (Fig. 3b). This value was typically less than ~2‰ over 24 h. If substantial drift (>1‰) was observed over the course of a run, data were corrected by assuming a constant drift during the analysis. In no case did this noticeably alter the isotopic trends observed in our incubations. As a second check, we oriented our sample analyses to provide an internal measure of instrument drift. This is especially important because of the substantial (~12–24 h) time between analysis of standards. For each run, analyses were organized into rectangular grids, which were aligned perpendicular to the mat surface and analyzed sequentially as indicated in Fig. 3a. As the primary trends of interest are those occurring as a function of depth beneath the mat surface, each grid of data was collected as a series of analyses oriented from shallow to deep and then deep to shallow within the mat, for a total of ~10 adjacent, parallel depth profiles. This resulted in multiple, independent transects in the direction of interest (half shallow to deep; half deep to shallow). Drift within the analysis would manifest itself as a lateral gradient superimposed on any depth variation. At the resolution of these analyses (~1‰), no such lateral (left–right) shift was observed in the isotopic composition of any of the samples. For example, in one incubation, two parallel $\delta^{34}S$ minima at 6 and 8 mm below the mat surface (Fig. 3c) occur in all 10 of the parallel depth profiles with no shift in $\delta^{34}S$ laterally across the grid. This lateral reproducibility (both against instrument drift and random variations within the sample) makes these 2-D grids a robust approach for mapping spatial variability in $\delta^{34}S$ at high resolution.

The $\delta^{34}S$ composition of sulfate from the Guerrero Negro mats was 21.0 ± 0.1‰ (i.e., seawater). The

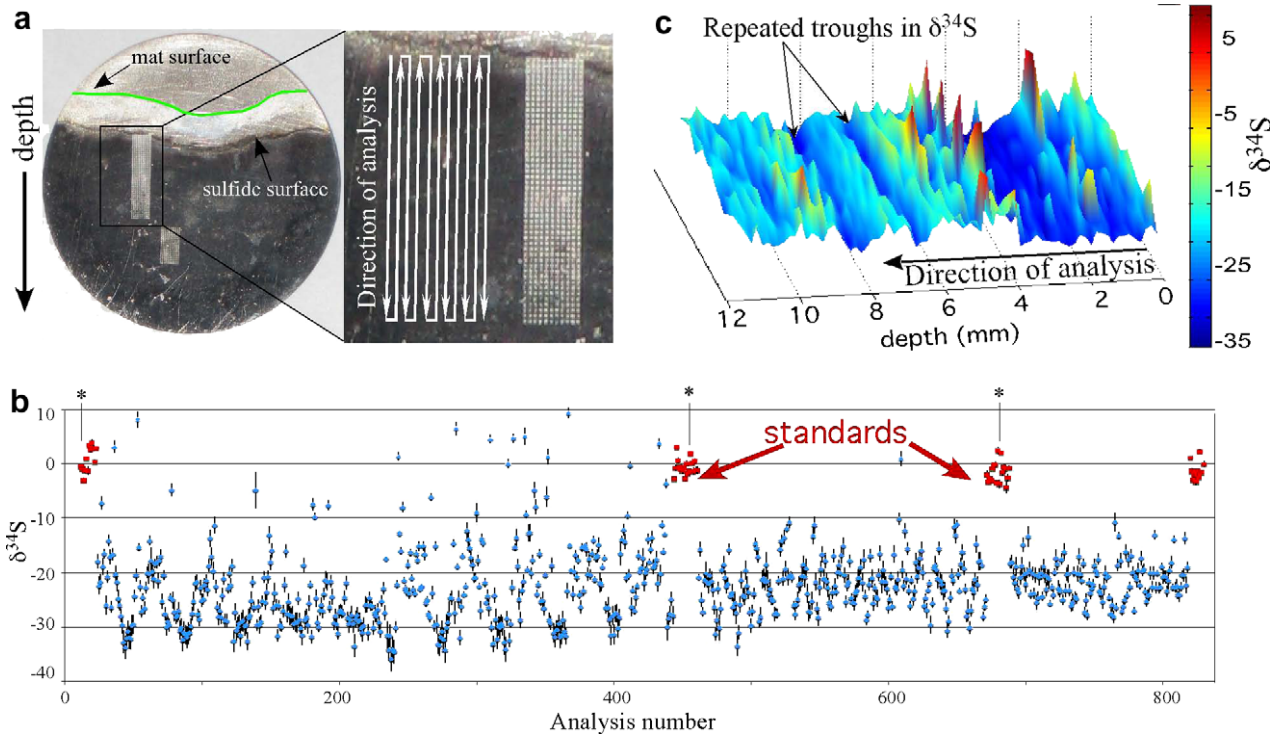

Fig. 3. Analytical approach. (a) Incubations were analyzed in 2D grids with the long axis oriented perpendicular to the mat surface (the disk shown is the daytime 80 mM incubation from the NASA Ames greenhouse). Analyses were run from shallow → deep, deep → shallow, etc., allowing for multiple independent $\delta^{34}S$ depth profiles beneath the mat. (b) $\delta^{34}S$ from sequential analyses of the Guerrero Negro nighttime field incubation (blue) with standards shown (red). *Indicates instrument recalibration between sets of standards. Vertical error bars represent the standard error ($n = 20$ cycles) for each measurement. There is significant variability when observing the analyses sequentially (b). However, when they are viewed spatially (c), the variation becomes more coherent. The x, y coordinates in (c) reflect the physical location on the disk where the measurements were made (i.e., in a 2D grid) and the height/color record the $\delta^{34}S$ value measured at that point. Note particularly that two local minima in $\delta^{34}S$ at 6 and 8 mm depth repeat in each of the ten parallel transects across the mat. Any instrument drift over the course of this run is insignificant compared to the ~10‰ variations in $\delta^{34}S$ into and out of these troughs. Note also that much of the apparent scatter of enriched $\delta^{34}S$ values observed in (b) are confined to a narrow depth zone near 4 mm.

incubations in the greenhouses at NASA Ames Research Center were conducted with an artificial brine, in which the sulfate $\delta^{34}S$ had a value of -0.7 ± 0.1‰. To directly compare the sulfide results from the Ames greenhouse with those from the field incubations, the resulting sulfide $\delta^{34}S$ from Ames were corrected to the values they would have had if the artificial seawater had the same isotopic composition as seawater ($\delta^{34}S_{SW}$). Briefly, the fractionation $\alpha = (\delta^{34}S_{Ames\text{-}SO4}/1000 + 1)/(\delta^{34}S_{sulfide}/1000 + 1)$ between Ames sulfate and observed (IMF-corrected) sulfide was determined. This fractionation was then used to determine the seawater-corrected $\delta^{34}S_{SC}$ value for the sulfide from the Ames incubations: $\delta^{34}S_{SC} = (\delta^{34}S_{SW}/1000 + 1)/\alpha$.

3.4. Fluorescence in situ hybridization (FISH)

The distributions of select sulfate-reducing bacterial groups were visualized by 16S rRNA-targeted fluorescence *in situ* hybridization and tyramide signal amplification (CARD-FISH) (Pernthaler et al., 2002). Here, whole-cell hybridization was performed on thin sections (15 μm thick) of mat spanning a vertical depth of ~12 mm. Mat samples were collected in parallel with silver disk incubations from the NASA Ames greenhouse and from the P4n5 field site. Cores of mats were collected using a 3 cm^3 disposable syringe with the tip removed and preserved in 2% paraformaldehyde as described in Fike et al. (2008). FISH hybridizations were conducted with the following HRP-labeled oligonucleotide probes (Biomers, Ulm, Germany): DSS 658 (targeting select members of the sulfate-reducing Desulfobacteraceae family (Manz et al., 1998)), DSV 687 (members of the Desulfovibrioaceae (Devereux et al., 1992)), and DSB 660 (targeting members of the Desulfobulbaceae (Devereux et al., 1992)). The fluorescent signal was subsequently amplified using a fluorescein-labeled tyramide as described in Fike et al. (2008). Cyanobacteria appear red under epifluorescence microscopy due to the autofluorescence of photosynthetic pigments. Mat sections were counter-stained with diamidino-2-phenylindole (DAPI), which binds to DNA. Slides were examined on a DeltaVision RT deconvolution microscope system (Applied Precision, Ithaca, WA, USA) with 20×, 40× or 60× Olympus objectives (PlanApo or UPlanApo). Images were cap-

tured and processed using the Softworx package (version 3.5.1; Applied Precision) and paneled images were exported as TIFFs for final figure assembly in Adobe Photoshop CS (Adobe Systems Incorporated).

When assembling composite FISH images that cover substantial (~50 mm^2) regions of the Guerrero Negro mats, there are often irregularities in mat thickness and the presence of small folds, leading to differential brightness in the image. To compensate for these variations in signal intensity, we set the blue (DAPI) channel to a constant value and scaled the red (cyanobacterial autofluorescence) and green (sulfate reducers of the Desulfobacteraceae, Fig. 8) accordingly in Matlab. Average depth profiles were created of the cyanobacterial and sulfate-reducing bacterial abundances from the image, which were then broadly compared with the fine-scale $\delta^{34}S$ isotope trends generated from SIMS analysis.

4. RESULTS

4.1. Field incubations at Guerrero Negro

4.1.1. Subtidal mats (80 mM SO_4)

During the day incubation in the subtidal mats at Guerrero Negro, the first visible accumulation of sulfide occurred approximately 2.7 mm below the mat surface (Fig. 2). The distance between the mat surface and onset of sulfide was maintained despite the undulatory surface of the mat. Visible banding on the disk was observed in the first mm of sulfide accumulation, after which sulfide levels precluded visual recognition of variation. Despite the lack of visible banding in the lower portion of the disk, variations were documented in the relative SIMS ^{32}S counts (right panel of Fig. 4). There is a pronounced $\delta^{34}S$ enrichment at the top of the chemocline (with values at −10 to

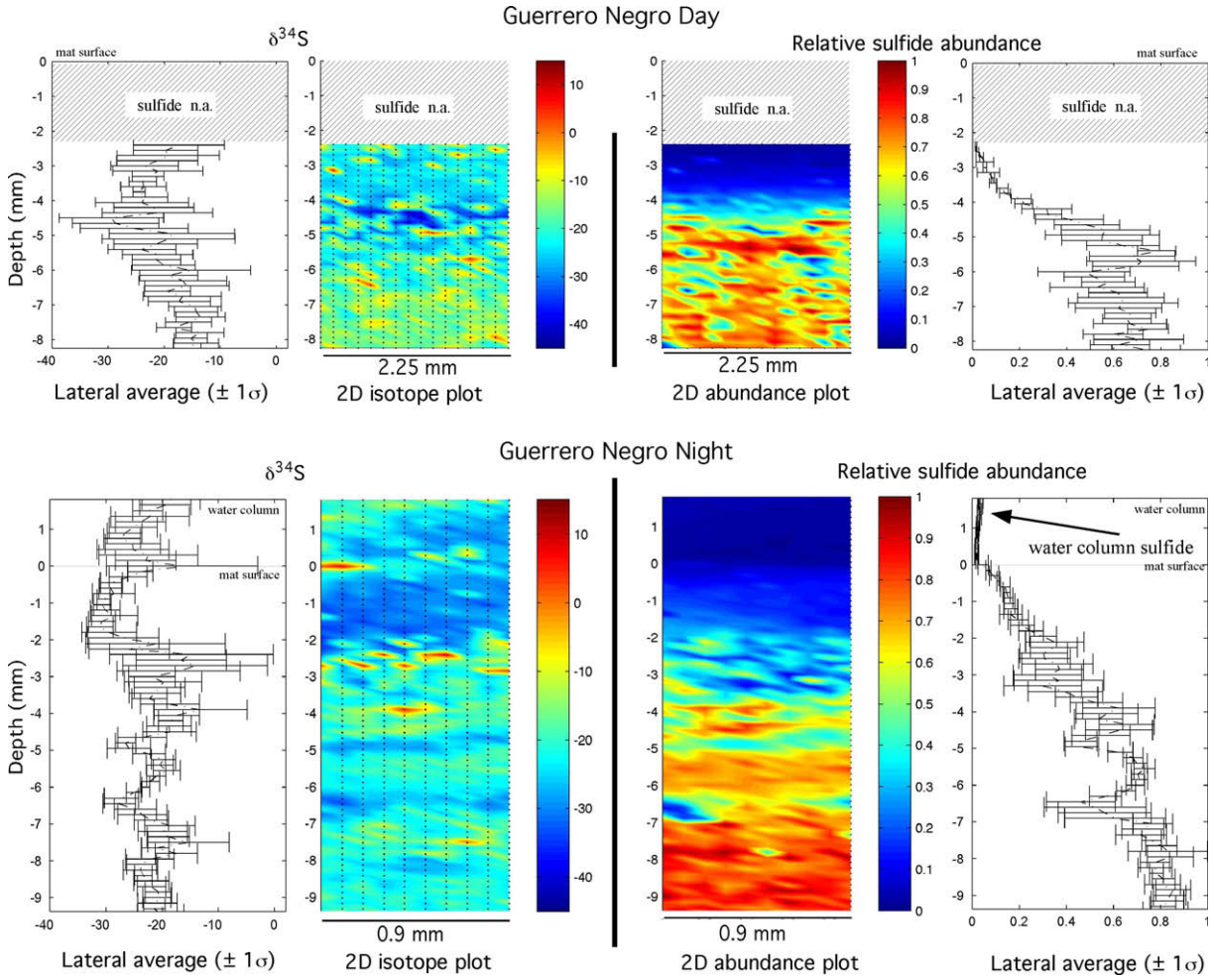

Fig. 4. SIMS data from Guerrero Negro field incubations. 2D grids are shown in the center with color corresponding to $\delta^{34}S$ on the left and sulfide yield (normalized relative to the maximum value in each incubation) on the right. Depth-averaged values are shown on the sides. Note the horizontal range in these depth-averaged graphs depicts the lateral variability (1σ standard deviation of values) for a given depth and not errors on the measurements (which are ~1‰). Here and in subsequent figures, the *y*-axis indicates depth beneath the mat surface. The analysis of the day and night incubations starts at correspondingly different depths due to the diurnal vertical migration of the sulfide gradient. Note that in the night incubations, the analyses extended into the water column to measure the sulfide captured there (see Fig. 2). n.a. = Not analyzed.

−20‰, ~2.3 mm below the mat surface). With depth $\delta^{34}S$ values decrease to a minimum value around −35‰ at 4.5 mm below the mat surface, before rising again toward −10‰ approximately 8 mm below the mat surface.

During the night incubation, the zone of sulfide accumulation migrated upward to just below the mat/water interface, reflecting the vertical shift in the chemocline caused by the end of daylight photosynthetic activity (Figs. 2 and 4). Sulfide precipitation on the disk highlights the irregular topography of the mat surface. Additionally, sulfide was observed to template onto the silver disk from within the water column. However, no visible sulfide deposition occurred at the mat surface itself (Fig. 2), suggesting rapid sulfide oxidation at this interface. This is seen in the ^{32}S sulfide counts in Fig. 4. The sulfide in the water column at night has similar $\delta^{34}S$ values (−25 to −20‰) to that recorded in the surface layers of the mat and may have been sourced from sulfide diffusing from the mat or perhaps from active sulfate reduction in the water column, particularly within the diffusive boundary layer overlying the mat (Jorgensen and Des Marais, 1990). Sulfate levels are sufficiently high in these mats (80 mM), relative to maximum sulfide levels (~500 μM), to preclude any enrichment in the residual sulfate $\delta^{34}S$ with depth due to ongoing sulfate reduction (which could, in turn, affect the measured sulfide $\delta^{34}S$). Similar to the day incubation, there is an enrichment in $\delta^{34}S$ at the top of the chemocline (the mat surface), where values average ~−20‰. $\delta^{34}S$ decreases with depth down to −30‰ at ~1.5 mm below the surface, and subsequently increase back toward −15‰ at ~2.5 mm below the mat surface. Further $\delta^{34}S$ oscillations between −15‰ and −30‰ occur with depth down to ~1 cm below the mat surface.

The absolute values of $\delta^{34}S$ observed in the day and night incubations were similar, including the $\delta^{34}S$ enrichments in the chemocline. Two depleted $\delta^{34}S$ bands (down to ~−30‰) are prominent in the night incubation at ~5 mm and 6.2 mm depth. Similarly spaced depletions in $\delta^{34}S$ to ~−30‰ also occur at ~4.5 and ~5.5 mm during the day incubations, suggesting that $\delta^{34}S$-banding may be ubiquitous at depth and spatially invariant over day/night cycles when located sufficiently deep below the chemocline. The uncertainty in the exact position of the mat/water interface in our analysis caused by irregularities in the mat surface (up to 1 mm variation in topography) may be responsible for the offset in the $\delta^{34}S$ bands observed in the day and night incubations.

4.2. Ames greenhouse incubations

4.2.1. Incubation at 80 mM SO_4

Mats were maintained in the greenhouse flume system in an artificially-prepared brine for 17 months prior to silver disk incubation to ensure adequate time for microbial mat equilibration with the laboratory environment. During the day incubation of 80 mM sulfate mat in the greenhouse, the first visible accumulation of sulfide occurred 2.4 mm below the mat surface, and again tracked the slightly irregular mat surface (Fig. 2c). Similar to the field incubation, visible banding occurred in the upper mm of the sulfidic zone during the day incubation. Oxygen microelectrode profiles (Fig. 5a) show that the chemocline migrated approximately 3 mm over the diurnal cycle. This can be seen by the vertical migration toward the mat surface of the visible sulfide accumulation during the night incubation, similar to trends previously documented in other microbial mats (Revsbech et al., 1983). No substantial sulfide precipitation occurred at or above the mat water interface during the night incubation. The difference between this greenhouse incubation (no water-column sulfide) and the field night incubation (water-column sulfide) likely arises from the fact that the flowing water in the greenhouse flume maintains equilibrium between atmospheric oxygen and the water overlying the mats.

SIMS analysis of the 80 mM day incubation revealed that the uppermost zone of sulfide accumulation is substantially enriched in $\delta^{34}S$ with respect to lower layers. From the upper sulfide zone, $\delta^{34}S$ drops sharply by ~15‰ between 3–4 mm below the mat surface, followed by a more gradual decrease for another 3 mm. At greater depths, $\delta^{34}S$ displayed significant variations, becoming alternately more enriched from 7–10 mm ($\delta^{34}S \sim -15‰$) and 11–12 mm ($\delta^{34}S \sim -25‰$) and more depleted ($\delta^{34}S \sim -35‰$ from 10–11 and 12–14 mm). During the night incubation, $\delta^{34}S$ values showed a similar trend with enriched values in the uppermost sulfidic layers and a sharp and then more gradual depletion in $\delta^{34}S$ over the next 3 mm. As observed with the mat incubations in the field, the absolute values of $\delta^{34}S$ observed in the greenhouse day and night incubations were similar.

4.2.2. Incubation at 1 mM SO_4

During the day incubation at 1 mM SO_4, the first visible accumulation of sulfide occurs 2.4 mm below the mat surface, while visible sulfide accumulation occurs just below the mat surface during the night incubation (with no substantial sulfide deposits at or above the mat surface) (Fig. 2c). This distance is consistent with the migration of the oxygen profiles (Fig. 5b) over the diurnal cycle. Significantly less sulfide templated out on the disk during these incubations than the 80 mM sulfate incubations (Fig. 2b). There is a peak in sulfide concentration just below the mat surface and sulfide concentration decreased at depth below this level, observed both visually and in the SIMS data (Fig. 5b). This trend was not observed in other incubations (at high sulfate concentrations) and likely reflects rapid sulfate reduction rates in the upper sulfidic zone. In these incubations, it is possible that a substantial portion of the original sulfate pool is consumed at depth. Depending on the fractionation associated with sulfate reduction in the upper portion of the mat, this may result in an isotopic enrichment in the remaining sulfate (and potentially sulfide) in the deeper layers of the mat.

The apparent fractionations between sulfate–sulfide in these incubations (~30‰, Fig. 5b) are much smaller than those in the 80 mM incubations (both field and in the Ames greenhouse), where fractionations typically reached ~50‰. In addition, there was much less $\delta^{34}S$ variability in these 1 mM incubations (ranging from −20‰ to 0‰) than in either of the 80 mM incubations (Fig. 5b). The main zone of variability is represented by a 5‰ enrichment in $\delta^{34}S$

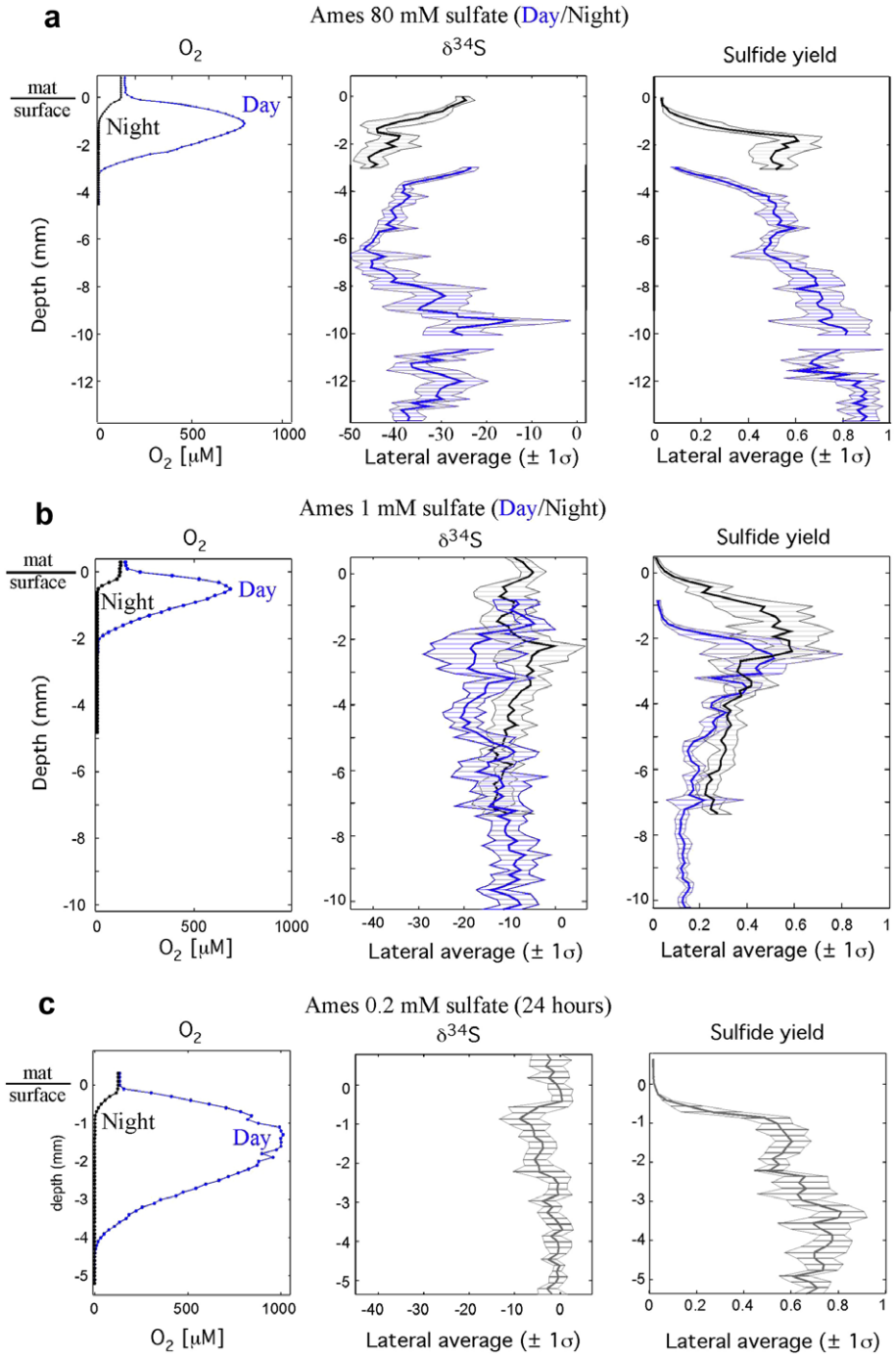

Fig. 5. Paired oxygen microelectrode data (left) and SIMS data ($\delta^{34}S$ in center and normalized sulfide yield on the right) from the greenhouse incubations at NASA Ames Research Center. The depth of the chemoclines in the individual incubations varied laterally and no consistent differences were observed between the different incubations. Note the horizontal range for the SIMS data in these depth-averaged graphs depicts the lateral variability (1σ standard deviation of values) for a given depth. Photosynthesis causes a strong diurnal migration of redox gradients within the mat. (a) 80 mM SO_4 day (blue) and night (black) incubations. Isotope enrichments are observed in the upper sulfidic layers during both the day and night incubations (center). The migration of the redox front results in a vertical shift in the sulfide zone but no change in its isotopic composition or gradient with depth. Significant sulfide $\delta^{34}S$ variations occur at depths up to 1.5 cm below the mat surface. Sulfide concentrations increase over the first ~2 mm, followed by smaller variations at greater depths. No data were collected from the day incubation disk between 10 and 10.8 mm below the mat surface (see Fig. 2). (b) 1 mM SO_4 day (blue) and night (black) incubations. There is less $\delta^{34}S$ variability in these incubations than in (a). A pronounced ~5‰ enrichment is visible across the chemocline in both day and night incubations. Peaks in sulfide yield indicate elevated sulfate reduction rates just beneath the chemocline (~1–2 mm during the day and ~2–3 mm during the night). (c) 0.2 mM incubation (24 h). $\delta^{34}S$ show the little variation (total range ~10‰) and lateral variability is on the same scale as the changes in $\delta^{34}S$ with depth. A pronounced ~5‰ enrichment across the chemocline is also observed in this incubation.

at and above the first layer of visible sulfide accumulation (at ~2 mm depth (day) and ~0.5 mm depth (night)).

4.2.3. Incubation at 0.2 mM SO_4

Sulfide levels in the 0.2 mM SO_4 incubation were sufficiently low that only a single 24-h (day/night) incubation was conducted. Observed fractionations for this incubation (20–25‰; Fig. 5c) were slightly less than those observed in the 1 mM incubations (~30‰) and there was little variability in $\delta^{34}S$ with depth, except for a small enrichment (~5‰) at the top of the zone of visible sulfide accumulation (0.5 mm depth). Note that because of the long (24 h) incubation in this 0.2 mM experiment, the diurnal vertical migration of the chemocline (4 mm) may have smoothed any spatial signals in $\delta^{34}S$ or sulfide yield in the upper several mm.

4.3. Diffusion and abiotic oxidation experiments

Analysis of our diffusion experiments (Fig. 6) revealed that sulfide concentrations in the upper portion of the agar had decreased substantially and sulfide was detected in the water column immediately above the agar (decreasing in abundance with distance from the agar surface). Agar $\delta^{34}S$ was approximately uniform at depth with a slight enrichment (~2‰) in the upper agar approaching the contact with the water column, presumably caused by the preferential diffusion of ^{32}S out of the agar. A corresponding depletion in $\delta^{34}S$ of sulfide trapped from the water column was observed. Similar variations (a few permil enrichments and depletions in the upper agar layers and in the overlying water column, respectively) were observed in the anoxic incubation at pH 7 (Fig. 6a) and those conducted with agitated oxic water at pH 7 (Fig. 6b) and pH 8 (Fig. 6c), as well as the other control experiments conducted. These data indicate that the effects of diffusion, abiotic oxidation, and pH change may only account for minor shifts in $\delta^{34}S$ and are not plausible explanations for the large amplitude variations (>>10‰) that we observe in the microbial mat incubations.

4.4. FISH experiments

As a first step in trying to assess the factors influencing patterns of $\delta^{34}S$ distribution within the *Microcoleus* mats, we characterized the spatial distribution of some of the major sulfate-reducing bacterial groups as a function of depth within the mat using fluorescence *in situ* hybridization (FISH). CARD-FISH analysis with a general probe targeting members of the Desulfobacteraceae (DSS 658) revealed a thick (ca. 1 mm) horizontal band of abundant long filamentous Desulfobacteraceae cells at or just below the main concentration of autofluorescent cyanobacteria (Fig. 7). This banding pattern near the surface layers of the mat was observed in both field collected and greenhouse maintained microbial mats (80 and 1 mM SO_4 treatments). The cells had a morphology that is reminiscent of members of the *Desulfonema* genus (Fukui et al., 1999), a group targeted by the DSS 658 probe and known to be oxygen tolerant (Teske et al., 1998). Additional CARD-FISH experiments using probes targeting members of the Desulfobulbaceae (DSB 660) and Desulfovibrioaceae (DSV 687) also yielded positively hybridized cells, however the abundance of these groups relative to the Desulfobacteraceae was low and their distribution in replicate samples more heterogeneous, making it difficult to interpret any

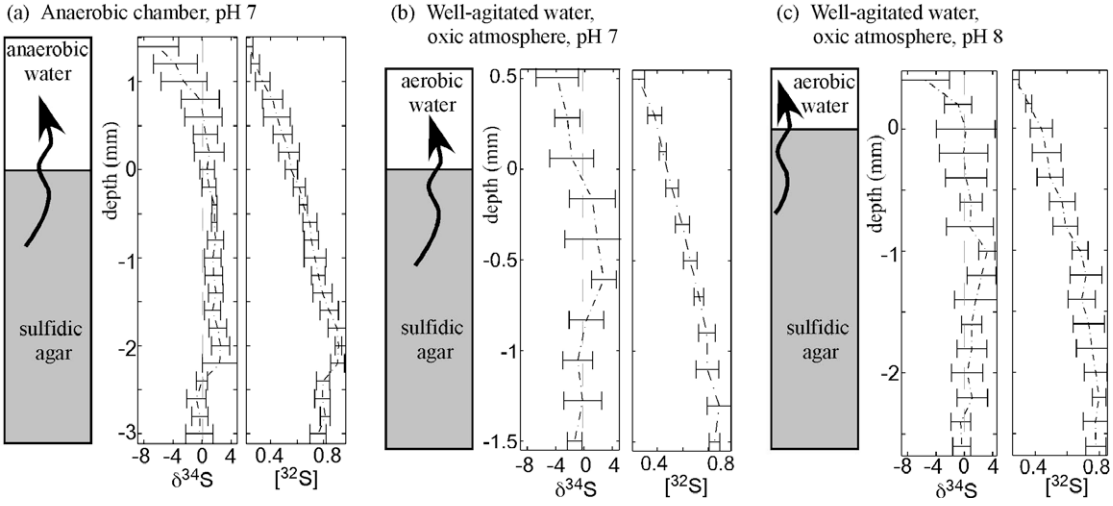

Fig. 6. SIMS data from abiotic diffusion experiments. For each, an experimental schematic is shown at left, followed by $\delta^{34}S$ and sulfide yield, respectively. (a) Anaerobic (N_2-purged) overlying water with sulfidic (pH 7) agar, conducted in an anaerobic chamber. A small enrichment in $\delta^{34}S$ in the residual sulfide in the upper layers of agar was observed, along with a corresponding $\delta^{34}S$ depletion in sulfide trapped from the water column. (b and c) Agitated (air-bubbled) overlying water with sulfidic (pH 7 (b) and pH 8 (c)) agar, conducted on the lab bench. A similar enrichment in $\delta^{34}S$ in the residual sulfide in the upper layers of agar was observed, as well as a depletion of the same magnitude in the sulfide trapped from the water column. The resulting enrichments in the upper layers of the agar and depletions in overlying water column result in small (~2–4‰) shifts away from the baseline $\delta^{34}S$ value. Note that the trend toward depleted values upward across the 'chemocline' in these experiments is opposite the $\delta^{34}S$ enrichment observed across the chemocline in the mat incubations.

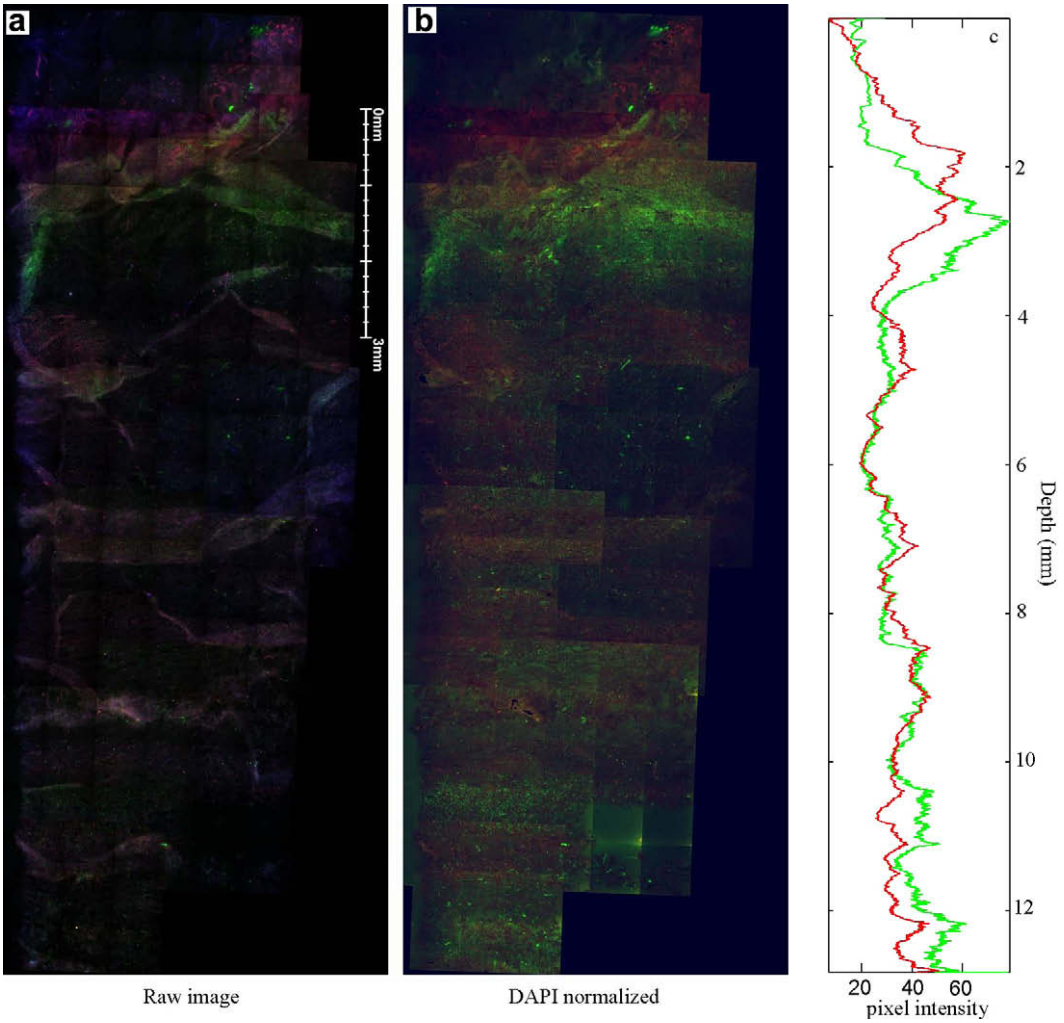

Fig. 7. Composite low magnification (10×) CARD-FISH image showing the distribution of Desulfobacteraceae hybridized with probe DSS 658 (in green) within the 80 mM SO_4 mat from a sample collected at 6 AM. The red signal is from cyanobacterial autofluorescence and the blue signal is the DNA stain DAPI. Scale bar is 3 mm and total imaged area of mat is ca. 10 mm deep by 5 mm wide. (a) Raw image composite. The irregular bright zones are areas where the mat has folded in upon itself. (b) The same image as in (a), but here normalized to a constant intensity in the blue channel (to mitigate the effects of folding). (c) Depth average of cyanobacterial autofluorescence in red and DSS sulfate.

general trends regarding their distribution in the mat. The dominance of Desulfobacteraceae within the chemocline is consistent with previous studies both from the Guerrero Negro site and other locations using non-microscopy-based molecular detection methods (Risatti et al., 1994; Minz et al., 1999a,b; Fourcans et al., 2006). Earlier studies additionally reported the presence of *Desulfovibrio* in the upper layers of the mat (Risatti et al., 1994). The discrepancy between previous rRNA-based abundance estimates and the limited detection of *Desulfovibrio*-affiliated cells by CARD-FISH is not understood at this time; it is possible that the probe and hybridization conditions need further optimization for successful detection of members of this group within the microbial mat.

The mat CARD-FISH hybridization shown in Fig. 7 was collected before dawn (6 AM) and represents a nighttime incubation. There was a sharp boundary approximately 1–1.5 mm from the mat surface marking the uppermost zone of the sulfate-reducing Desulfobacteraceae cells. By comparing the average channel brightness (0–255) in the FISH images (Fig. 7), we can get a sense of the depth distribution of cyanobacteria (in red) and select sulfate-reducers (those targeted by the DSS 658 probe, in green). To minimize the effects of variable mat thickness in the raw FISH composite images (Fig. 7a), we used an image that has been normalized to a constant value in the blue channel, corresponding to the DAPI DNA stain (Fig. 7b). A plot of the resulting depth-averaged pixel values (0–255) revealed a broad peak in the abundance of cyanobacteria in the upper 3 mm, which corresponded to the oxic zone during daytime photosynthesis (Fig. 5a). A dense band of Desulfobacteraceae cells partially overlapped with the peak in cyanobacterial autofluorescence, approximately 1.5–2.5 mm below the mat surface in the nighttime

incubation. While this is the most visually significant band of sulfate-reducing Desulfobacteraceae in all treatments (high and low SO_4 incubations), deeper layers in the mat also harbored distinct distribution patterns of this group, with discrete mat layers supporting greater concentration of hybridized cells relative to surrounding horizons. In Fig. 7, bands of Desulfobacteraceae-affiliated cells below the chemocline were apparent at approximately 6.5, 8.5, 9.8 and 10.5–11 mm. A direct correlation between the FISH data and microscale sulfide isotope distribution is not possible at this time, however it is worth noting that the ~mm spacing of these deeper layers, and those reported previously (Fike et al., 2008) is of the same magnitude as the variability in $\delta^{34}S$ observed with depth (Figs. 4 and 5).

5. DISCUSSION

5.1. $\delta^{34}S$ enrichment near the mat surface

The surface photosynthetic layers and underlying chemocline represent the most dynamic and productive horizons of the microbial mat, supporting high levels of microbial diversity and biomass relative to permanently anoxic underlying layers (Ley et al., 2006; Jahnke et al., 2008). This ~3–4 mm zone is also defined by steep photosynthetically controlled redox gradients and elevated rates of microbial activity, including some of the highest levels of bacterial sulfate reduction on record (Visscher et al., 1992; Canfield and Des Marais, 1993; Baumgartner et al., 2006; Dillon et al., 2007). Examination of the trends in sulfide $\delta^{34}S$ across this dynamic horizon revealed significant isotopic enrichments (~15–20‰) in the upper mm of sulfide accumulation during both the day and night incubations conducted in the field and at 80 mM SO_4 in the Ames greenhouse. These represent the suite of samples with surplus sulfate, where distillative enrichment of sulfate $\delta^{34}S$ (and thereby sulfide) with depth can be excluded. A similar trend represented by smaller $\delta^{34}S$ enrichments (5‰) was also observed in the upper layers of the 1 mM SO_4 (day and night) and in the 0.2 mM SO_4 mat incubations (Fig. 5). While sulfate limitation may influence the magnitude of the sulfide $\delta^{34}S$ recorded in these greenhouse incubations, the general enrichment pattern observed within the chemocline is opposite from the trend predicted by progressive consumption of the sulfate pool (increasing $\delta^{34}S$ with depth as the sulfate pool is partially consumed). As such, the $\delta^{34}S$ enrichments recorded in these silver disk incubations represent a minimum estimate of the true change in fractionation.

There are several factors that could influence $\delta^{34}S$ trends at the chemocline, including diffusion, abiotic or biotic sulfide oxidation, sulfur disproportionation, and changing fractionation during sulfate reduction. Sulfur cycling within the mats is inherently complex and it is possible that all of these factors may influence the resulting sulfide $\delta^{34}S$ pool to varying degrees. However, existing microbiological and geochemical data (Canfield and Des Marais, 1993; Bebout et al., 2004) suggest that the observed enrichment in $\delta^{34}S$ is likely due to enhanced microbial activity within the chemocline, specifically driven by elevated sulfate reduction rates and substantial re-oxidation of newly produced sulfide, rather than physico-chemical variability. Both of these processes will contribute toward decreased sulfate–sulfide fractionations and therefore an enrichment in sulfide $\delta^{34}S$ (Fig. 1). Below we explore each of these possible mechanisms for generating the observed sulfide $\delta^{34}S$ enrichment at the chemocline.

Experiments designed to examine the $\delta^{34}S$ fractionation associated with diffusion, abiotic sulfide oxidation, and pH, were shown to have a relatively minor influence on the variation in $\delta^{34}S$ (Fig. 6) and are unlikely to account for the magnitude of enrichment measured in the surface layers of the mat (Figs. 4 and 5). Control experiments using sulfide-impregnated agar (approximating the consistency of the gelatinous mat) and overlain by oxic or anoxic water maintained at pH 7 or 8 consistently showed $\leqslant$3–4‰ variation in $\delta^{34}S$, adjacent to the mat/water interface, independent of treatment. In addition, these diffusion-dominated trends (increasingly ^{34}S-depleted above the 'chemocline') are opposite that observed from our mat incubations (increasingly ^{34}S-enriched above the chemocline. These findings are consistent with reports from independent studies showing only small fractionation between sulfate and sulfide $\delta^{34}S$ associated with abiotic sulfide oxidation (Fry et al., 1986b, 1988b; Habicht et al., 1998; Canfield, 2001a). Explanations of this mm-scale $\delta^{34}S$ enrichment that rely on changes in physical factors (e.g., temperature, or salinity) (Arnosti et al., 1998; Sagemann et al., 1998; Canfield et al., 2006; Hoek et al., 2006; Porter et al., 2007; Finke and Jorgensen, 2008), or sulfate concentrations (Habicht et al., 2002) within the individual mat incubations can also be ruled out. At nearly 3 times seawater concentrations, sulfate levels are non-limiting for both the field and 80 mM greenhouse mats and localized depletion in sulfate concentration (and resulting enrichment in $\delta^{34}S$ due to distillation) is insufficient to account for the change in sulfide $\delta^{34}S$ observed.

Other possible factors that could cause this isotopic enrichment are changes in electron donor or in sulfate reduction rate (Fig. 1). The use of hydrogen or organic carbon as the electron donor during sulfate reduction can impact fractionation during BSR, with use of hydrogen associated with decreased isotopic fractionations (Canfield, 2001a). Generation of H_2 is associated with photosynthesis and respiration within the upper surface of the mats (Hoehler et al., 2002). A switch from BSR predominantly associated with H_2 utilization in the upper chemocline to organic carbon respiration in the deeper layers of the mat could explain the $\delta^{34}S$ enrichment observed in this zone. However, if H_2-coupled sulfate reduction is in part responsible for the enrichment in $\delta^{34}S$, this process appears to be insensitive to the substantial diurnal variation in the *in situ* H_2 concentration (Hoehler et al., 2002), as the magnitude of enrichment was consistent in both the day and night incubations.

Similar to the differences in fractionation between H_2- and organic carbon-utilizing BSR, ^{34}S-fractionation during BSR can vary based on different sources of organic carbon (e.g., acetate vs. lactate) (Canfield, 2001a). Differential carbon availability has been considered a likely candidate for regulating sulfate reduction in these mats because of the diurnal oscillation between photosynthesis- and

respiration-dominated metabolic cycles. The availability of excess photosynthate (organic compounds synthesized during photosynthesis) during the day may explain the occurrence of sulfate-reducing bacteria within the oxic upper layers of the mats (Minz et al., 1999b; Baumgartner et al., 2006) and the observed close physical association between the *Desulfonema*-like sulfate-reducing bacteria and filamentous cyanobacteria (Fig. 8).

A change in the composition and relative activity of microbial metabolisms (e.g., sulfate reduction, sulfur disproportionation, sulfide oxidation) involved in sulfur cycling can significantly alter the fractionation between coexisting sulfate and sulfide $\delta^{34}S$ (Fry et al., 1984, 1985, 1986a, 1988a; Canfield and Thamdrup, 1994; Canfield and Teske, 1996; Canfield et al., 1998; Habicht et al., 1998; Canfield, 2001a). For example, sulfur disproportionation typically leads to increased isotopic fractionation between sulfate and sulfide (Canfield and Thamdrup, 1994; Canfield et al., 1998; Habicht et al., 1998). Disproportionation reactions are most likely to occur in the chemocline itself, where redox gradients allow for the creation of intermediate sulfur species (Jorgensen, 1994). However, the increased fractionation in sulfide $\delta^{34}S$ predicted from disproportionation is opposite from the isotopic enrichment observed in the chemocline (Habicht et al., 1998).

Sulfate reduction rates are also known to impact the fractionation during sulfate reduction (Fig. 1). Specifically, elevated sulfate reduction rates, such as are observed in and above the chemocline of microbial mats (Baumgartner et al., 2006) are typically associated with decreased fractionation during BSR, especially when organic carbon sources are used as electron donors (Canfield, 2001a). Decreased fractionation during BSR would manifest itself as an enrichment in sulfide $\delta^{34}S$, such as observed in our incubations (Figs. 4 and 5). High sulfate reduction rates occur at and above the chemocline in the Guerrero Negro mats during both the day and night (Canfield and Des Marais, 1993)

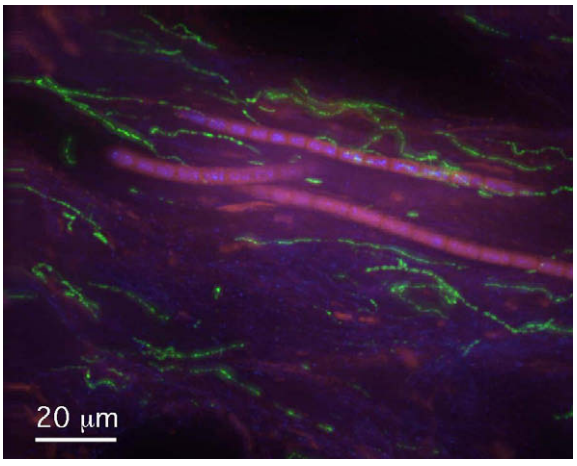

Fig. 8. CARD-FISH image of the upper mat section (ca. 1.5 mm beneath the mat surface) highlight the physical association of cyanobacteria (red, chlorophyll autofluorescence) and sulfate reducers (green, DSS 658 probe), which morphologically resemble the genus *Desulfonema*. Blue indicates the DNA stain DAPI.

in association with abundant microorganisms related to the sulfate-reducing Desulfobacteraceae and other groups in and above the chemocline (Figs. 7 and 8) (Risatti et al., 1994; Fike et al., 2008). Abundant SRBs at or above the chemocline, as observed in this study and reported by others (Risatti et al., 1994; Krekeler et al., 1997, 1998; Minz et al., 1999a,b; Sigalevich et al., 2000; Wieringa et al., 2000; Baumgartner et al., 2006; Fike et al., 2008; Fourcans et al., 2008), and the extremely elevated sulfate reduction rates occurring in these layers with respect to those in the strictly anoxic underlying strata (Frund and Cohen, 1992; Canfield and Des Marais, 1993), strongly suggest that enhanced activity by sulfate-reducing assemblages within the chemocline is influencing the sulfide signature (i.e., enriched $\delta^{34}S$) measured within this dynamic zone.

In addition to the potential effects from elevated sulfate-reduction rates, enhanced biological oxidation within this zone may also lead to $\delta^{34}S$ enrichment in the residual sulfide pool (Kaplan and Rittenberg, 1964; Fry et al., 1984, 1986a, 1988a). Both phototrophic and chemotrophic sulfide-oxidizing microorganisms are active within the upper mat layers (Cohen et al., 1975, 1986; Jorgensen and Des Marais, 1986; Castenholz et al., 1991; Dannenberg et al., 1992; Fuseler et al., 1996), and many of these, like the anoxygenic phototrophs, reside within or immediately below the oxycline (Fourcans et al., 2006). Members of the large sulfide-oxidizing gammaproteobacteria (e.g. *Beggiatoa*) are also common within this zone and can migrate over the course of the diurnal cycle (Hinck et al., 2007). Additionally, members of the dominant mat building cyanobacterial group (*Microcoleus chthonoplastes*) have also been shown to oxidize sulfide to thiosulfate in the light through anoxygenic photosynthesis (Jorgensen et al., 1986; de Wit and van Gemerden, 1987). The juxtapositioning of members of the sulfate-reducing Desulfobacteraceae with *Microcoleus*-like cyanobacterial filaments suggest the possibility of accelerated sulfur cycling (e.g., through anoxygenic sulfide oxidation) over short (~μm) spatial distances (Figs. 7 and 8). Currently, it is not possible to properly evaluate biotic sulfide oxidation as the source of the observed chemocline $\delta^{34}S$ enrichment because the fractionations associated with this biotic oxidation, while small, remain poorly constrained (Fry et al., 1984, 1985, 1986a, 1988a; Habicht et al., 1998; Canfield, 2001a). The comparable trend in $\delta^{34}S$ enrichment observed both in the day and night incubations (Figs. 4 and 5), however, suggests that if biological oxidation plays a role, the sink for sulfide is constant over the diurnal cycle, independent of oxygen and light, and capable of rapidly responding to the changing vertical position of the redox gradient in the mat. Similarly, while photosynthesis modulates the vertical position of the chemocline and thus, the base of the $\delta^{34}S$ enrichment zone, it has no direct impact on the magnitude of the $\delta^{34}S$ enrichment observed in the upper sulfidic zone of these photosynthetic mats.

In summary, elevated sulfate reduction rates are inferred to be the likely cause of the $\delta^{34}S$ enrichment we observe in the uppermost zone of sulfide accumulation within and above the chemocline, possibly magnified by intense biological scavenging/oxidation of sulfide by phototrophic and chemosynthetic microorganisms (e.g., *Microcoleus,*

Beggiatoa or anoxygenic phototrophs) operating both during the day and at night. High-resolution (sub-mm) studies of sulfate reduction rates using radiolabel ^{35}S in parallel with silver disk incubations may assist in further constraining probable cause of the $\delta^{34}S$ enrichment within this unique mat horizon.

5.2. Coherent $\delta^{34}S$ banding at depth

In addition to the $\delta^{34}S$ enrichments observed in the upper few mm of the mat, there are also variations in $\delta^{34}S$ of equal or greater magnitude deeper within the mats in both the field incubations and the 80 mM SO_4 Ames incubations in the NASA Ames greenhouse (Figs. 4 and 5). These variations are found up to depths of at least 1.5 cm below the mat surface and occur in both day and night incubations. Unlike the upper portion of the mats (above), no day/night difference is expected at these depths since they are deep enough not to be impacted by the diurnal photosynthetic forcing. The majority of the $\delta^{34}S$ variation at depth is found perpendicular to the mat surface (i.e., vertical rather than horizontal changes in $\delta^{34}S$) (Figs. 4 and 5). This variation at depth, presumably decoupled from the mat surface, is surprising; the sharp redox gradients at the mat surface are thought to be the primary driver of microbial metabolic activity within the mats. However, the significant $\delta^{34}S$ gradients ($\sim$20‰ over as little as 1 mm) observed at depth must arise *in situ* from the differential expression of microbial metabolic activity. Diffusion over time would eliminate both relict *in situ* isotope gradients and any arising through transport of sulfide from the surficial mat layers. It is difficult to *a priori* identify the cause(s) of these large, spatially-organized and frequent variations at depth: what environmental gradients are sufficiently steep at 1 cm below the mat surface to give rise to such a range in isotopic fractionation?

The observed variation in distribution and abundance of members of the Desulfobacteraceae at depth suggests that there is the potential for stratification in at least some of the sulfate-reducing bacterial assemblages throughout the mat and this may be one possible source for the variable fractionation in sulfide recorded in the deeper mat horizons. While not directly targeted in this study, members of the acetate-utilizing *Desulfobacter* have been reported to increase in abundance in the deeper mat layers and may also contribute to the variations observed in sulfide $\delta^{34}S$ at depth (Risatti et al., 1994). Several of the factors (e.g., type of carbon source and/or organic carbon availability) that are thought to play a role in sulfur fractionation are likely to also impact SRB population densities. Whether this relationship is direct (e.g., population density affecting sulfate reduction rate or substrate availability and, therefore isotopic fractionation during bacterial sulfate reduction) or indirect (both the population density and the isotopic fractionations reflect variations in another parameter), remains to be determined. However, these observations indicate that the deeper layers within these microbial mats remain ecologically and metabolically stratified and merit additional investigation. Until we can understand the spatial distribution of the relevant parameters (e.g., diversity, sulfate reduction rate, organic carbon and hydrogen availability, sulfur speciation) at an appropriately high resolution, we cannot fully assess the cause of the isotopic (and SRB population) variability that we document here.

5.3. The impact of SO_4 concentration on isotopic fractionation

In the field and greenhouse incubations with 80 mM SO_4, typical values for fractionation between sulfate and sulfide were 45–55‰, similar to values reported previously from laboratory incubations (Fike et al., 2008). The fractionation for these incubations varied by over 60‰, spanning the range from almost no fractionation to nearly 70‰. In contrast, the magnitude of fractionation observed in the 1 and 0.2 mM appeared to be substantially less ($\sim$15–30‰). Note, however, that given the low SO_4 concentrations in these incubations, we cannot rule out enrichment in sulfate $\delta^{34}S$ and thus a larger fractionation between sulfate–sulfide than is apparent from the initial sulfate $\delta^{34}S$. However, the lateral variability is less in these low sulfate incubations (rarely exceeding 10‰) than observed in the higher sulfate incubations, and is on par with the total vertical variations. The decreased lateral $\delta^{34}S$ variability in these low sulfate incubations (which is independent of the absolute value of $\delta^{34}S_{SO4}$) suggests that the parallel decrease in $\delta^{34}S$ variation with depth in these incubations is driven by decreased fractionation during BSR rather than any enrichment in sulfate $\delta^{34}S$ with depth. Previous investigation of bulk fractionation in microbial cultures has shown that fractionation during BSR is a function of ambient sulfate concentrations (Harrison and Thode, 1958; Canfield, 2001b; Habicht et al., 2002). For example, for sulfate concentrations below $\sim$0.1 mM, little to no fractionation was observed; whereas for sulfate concentrations above $\sim$1 mM fractionation generally increased with increasing sulfate concentrations (Habicht et al., 2002). Our data here show that these trends seem to hold in these complex environmental samples down to the 50 μm-scale.

These observations may provide additional constraints on the ancient sulfur cycle, particularly in Precambrian time, when there is significant uncertainty in the size of the sulfate reservoir (Brennan et al., 2004; Halverson and Hurtgen, 2007; Fike and Grotzinger, 2008; Hurtgen et al., 2009). One of the key proxies for the size of the marine sulfate reservoir is the fractionation between coeval sulfates and sulfides (Canfield, 2001a; Habicht et al., 2002; Hurtgen et al., 2005; Fike et al., 2006). However, through much of early Earth history, there are precious few direct records of sulfate $\delta^{34}S$, making it challenging to measure the true fractionation between sulfate and sulfide. If the small-scale variation in sulfide $\delta^{34}S$ can be related to the ambient sulfate concentration, the application of analyses like those presented here to sedimentary sulfides in the geologic record may improve our ability to constrain the size of the sulfate reservoir over Earth history.

6. CONCLUSIONS

We have documented the utility of 2D gridded analyses on a 7f-GEO SIMS in capturing small-scale ($\sim$100 μm–

1 cm) $\delta^{34}S$ variability in hydrogen sulfide produced within cyanobacterial mats from Guerrero Negro, Baja California Sur, Mexico. Investigations of daytime and nighttime incubations revealed that photosynthetic forcing had no detectable impact on observed near surface $\delta^{34}S$ patterns, which appear to be controlled by rapid sulfur recycling (elevated sulfate reduction rates coupled with enhanced sulfide oxidation) in the upper chemocline. Large, spatially-coherent oscillations ($\sim$20‰ over 1 mm) in $\delta^{34}S$ occurred at depths up to $\sim$1.5 cm below the mat surface. These gradients must arise from differential microbial fractionation during active production of sulfide, possibly arising from different microbial populations and/or metabolic levels, differential availability of carbon substrates, or additional sulfur species (e.g., polysulfides) at depth. Ambient sulfate concentrations were the dominant factor in determining the magnitude of fractionation (both vertical as well as lateral variability) associated with sulfide production. This suggests that small-scale $\delta^{34}S$ variations can be diagnostic for reconstructing past sulfate concentrations, even when the $\delta^{34}S$ of the initial sulfate pool is not known.

ACKNOWLEDGEMENTS

We would like to acknowledge the Gordon and Betty Moore Foundation and the Caltech Center for Geochemical and Cosmochemical Microanalysis for funding (to V.J.O.) as well as support from National Aeronautics and Space Administration grant NAI02-003-0001 issued through the Astrobiology Program and NASA grant 07-EXOB07-0093 issued through the Exobiology Program. D.A.F. was additionally supported by the Caltech O.K. Earl Postdoctoral Fellowship. N.F. was supported by an EU-Marie Curie Postdoctoral Fellowship Contract MOIF-CT-2005-22154. We would like to thank Y. Guan and J. Eiler for analytical assistance and invaluable discussions, and T. Lyons for conventional $\delta^{34}S$ analysis of aqueous sulfate. We are also indebted to the NASA Ames group (K. Turk, M. Kubo, L. Jahnke and D. Des Marais) for support and assistance with sample collections.

REFERENCES

Arnosti C., Jorgensen B. B., Sagemann J. and Thamdrup B. (1998) Temperature dependence of microbial degradation of organic matter in marine sediments: polysaccharide hydrolysis, oxygen consumption, and sulfate reduction. *Mar. Ecol. Prog. Ser.* **165**, 59–70.

Bak F. and Cypionka H. (1987) A novel type of energy-metabolism involving fermentation of inorganic sulfur-compounds. *Nature* **326**, 891–892.

Baumgartner L. K., Reid R. P., Dupraz C., Decho A. W., Buckley D. H., Spear J. R., Przekop K. M. and Visscher P. T. (2006) Sulfate reducing bacteria in microbial mats: changing paradigms, new discoveries. *Sedimentary Geol.* **185**, 131–145.

Bebout B. M., Carpenter S. P., Des Marais D. J., Discipulo M., Embaye T., Garcia-Pichel F., Hoehler T. M., Hogan M., Jahnke L. L., Keller R. M., Miller S. R., Prufert-Bebout L. E., Raleigh C., Rothrock M. and Turk K. (2002) Long-term manipulations of intact microbial mat communities in a greenhouse collaboratory: simulating Earth's present and past field environments. *Astrobiology* **2**, 383–402.

Bebout B. M., Hoehler T. M., Thamdrup B., Albert D., Carpenter S., Hogan M., Turk K. and Des Marais D. J. (2004) Methane production by microbial mats under low sulphate concentrations. *Geobiology* **2**, 87–96.

Berner R. A. (2006) GEOCARBSULF: a combined model for Phanerozoic atmospheric O_2 and CO_2. *Geochim. Cosmochim. Acta* **70**, 5653–5664.

Brennan S. T., Lowenstein T. K. and Horita J. (2004) Seawater chemistry and the advent of biocalcification. *Geology* **32**, 473–476.

Canfield D. E. (2001a) Biogeochemistry of sulfur isotopes. *Rev. Mineral. Geochem. Stable Isotope Geochem.* **43**, 607–636.

Canfield D. E. (2001b) Isotope fractionation by natural populations of sulfate-reducing bacteria. *Geochim. Cosmochim. Acta* **65**, 1117–1124.

Canfield D. E. and Des Marais D. J. (1993) Biogeochemical cycles of carbon, sulfur, and free oxygen in a microbial mat. *Geochim. Cosmochim. Acta* **57**, 3971–3984.

Canfield D. E., Habicht K. S. and Thamdrup B. (2000) The Archean sulfur cycle and the early history of atmospheric oxygen. *Science* **288**, 658–661.

Canfield D. E., Olesen C. A. and Cox R. P. (2006) Temperature and its control of isotope fractionation by a sulfate-reducing bacterium. *Geochim. Cosmochim. Acta* **70**, 548–561.

Canfield D. E. and Teske A. (1996) Late proterozoic rise in atmospheric oxygen concentration inferred from phylogenetic and sulphur-isotope studies. *Nature* **382**, 127–132.

Canfield D. E. and Thamdrup B. (1994) The production of S-34-depleted sulfide during bacterial disproportionation of elemental sulfur. *Science* **266**, 1973–1975.

Canfield D. E., Thamdrup B. and Fleischer S. (1998) Isotope fractionation and sulfur metabolism by pure and enrichment cultures of elemental sulfur-disproportionating bacteria. *Limnol. Oceanogr.* **43**, 253–264.

Castenholz R. W., Jorgensen B. B., Damelio E. and Bauld J. (1991) Photosynthetic and behavioral versatility of the cyanobacterium Oscillatoria–Boryana in a sulfide-rich microbial mat. *FEMS Microbiol. Ecol.* **86**, 43–58.

Chambers L. A., Trudinger P. A., Smith J. W. and Burns M. S. (1975) Fractionation of sulfur isotopes by continuous cultures of *Desulfovibrio desulfuricans*. *Can. J. Microbiol.* **21**, 1602–1607.

Claypool G. E., Holser W. T., Kaplan I. R., Sakai H. and Zak I. (1980) The age curves of sulfur and oxygen isotopes in marine sulfate and their mutual interpretation. *Chem. Geol.* **28**, 199–260.

Cohen Y. (1984) Comparative N and S cycles: oxygenic photosynthesis, anoxygenic photosynthesis, and sulfate-reduction in cyanobacterial mats. In *Recent Advances in Microbial Ecology* (eds. M. J. Klug and C. A. Reddy). American Society for Microbiology Press, Washington D.C.

Cohen Y. and Helman Y. (1997) Two-dimensional sub-millimetric mapping of sulfate reduction in marine sediments. *Am. Soc. Microbiol. 97th General Meeting, Abstr.* 393.

Cohen Y., Jorgensen B. B., Padan E. and Shilo M. (1975) Sulfide-dependent anoxygenic photosynthesis in a cyanobacterium Oscillatoria Limnetica. *Nature* **257**, 489–492.

Cohen Y., Jorgensen B. B., Revsbech N. P. and Poplawski R. (1986) Adaption to hydrogen-sulfide of oxygenic and anoxygenic photosynthesis among cyanobacteria. *Appl. Environ. Microbiol.* **51**, 398–407.

Cypionka H., Smock A. M. and Bottcher M. E. (1998) A combined pathway of sulfur compound disproportionation in Desulfovivrio desulfuricans. *FEMS Microbiol. Lett.* **166**, 181–186.

Dannenberg S., Kroder M., Dilling W. and Cypionka H. (1992) Oxidation of H-2, organic-compounds and inorganic sulfur-compounds coupled to reduction of O-2 or nitrate by sulfate-reducing bacteria. *Arch. Microbiol.* **158**, 93–99.

de Wit R. and van Gemerden H. (1987) Oxidation of sulfide to thiosulfate by *Microcoleus chtonoplastes*. *FEMS Microbiol. Lett.* **45**, 7–13.

Decker K. L. M., Potter C. S., Bebout B. M., Des Marais D. J., Carpenter S., Discipulo M., Hoehler T. M., Miller S. R., Thamdrup B., Turk K. A. and Visscher P. T. (2005) Mathematical simulation of the diel O, S, and C biogeochemistry of a hypersaline microbial mat. *FEMS Microbiol. Ecol.* **52**, 377–395.

Des Marais D. J., Cohen Y., Nguyen H., Cheatham M., Cheatham T. and Munos E. (1989) Carbon isotopic trends in the hypersaline ponds and microbial mats at Guerrero Negro, Baja California Sur, Mexico: implications for Precambrian stromatolites. In *Microbial Mats: Physiological Ecology of Benthic Microbial Communities* (eds. Y. Cohen and E. Rosenberg). American Society for Microbiology, Washington D.C..

Detmers J., Bruchert V., Habicht K. S. and Kuever J. (2001) Diversity of sulfur isotope fractionations by sulfate-reducing prokaryotes. *Appl. Environ. Microbiol.* **67**, 888–894.

Devereux R., Kane M. D., Winfrey J. and Stahl D. A. (1992) Genus- and group-specific hybridization probes for determinative and environmental studies of sulfate-reducing bacteria. *Syst. Appl. Microbiol.* **15**, 601–609.

Dillon J. G., Fishbain S., Miller S. R., Bebout B. M., Habicht K. S., Webb S. M. and Stahl D. A. (2007) High rates of sulfate reduction in a low-sulfate hot spring microbial mat are driven by a low level of diversity of sulfate-respiring microorganisms. *Appl. Environ. Microbiol.* **73**, 5218–5226.

Farquhar J., Johnston D. T., Wing B. A., Habicht K. S., Canfield D. E., Airieau S. and Thiemens M. H. (2003) Multiple sulphur isotopic interpretations of biosynthetic pathways: implications for biological signatures in the sulphur isotope record. *Geobiology* **1**, 27–36.

Fike D. A., Gammon C. L., Ziebis W. and Orphan V. J. (2008) Micron-scale mapping of sulfur cycling across the oxycline of a cyanobacterial mat: a paired nanoSIMS and CARD-FISH approach. *ISME J.* **2**, 749–759.

Fike D. A. and Grotzinger J. P. (2008) A paired sulfate–pyrite $\delta^{34}S$ approach to understanding the evolution of the Ediacaran–Cambrian sulfur cycle. *Geochim. Cosmochim. Acta* **72**, 2636–2648.

Fike D. A., Grotzinger J. P., Pratt L. M. and Summons R. E. (2006) Oxidation of the Ediacaran ocean. *Nature* **444**, 744–747.

Finke N. and Jorgensen B. B. (2008) Response of fermentation and sulfate reduction to experimental temperature changes in temperate and Arctic marine sediments. *ISME J.* **2**, 815–829.

Finster K., Liesack W. and Thamdrup B. (1998) Elemental sulfur and thiosulfate disproportionation by *Desulfocapsa sulfoexigens* sp. nov., a new anaerobic bacterium isolated from marine surface sediment. *Appl. Environ. Microbiol.* **64**, 119–125.

Fourcans A., Ranchou-Peyruse A., Caumette P. and Duran R. (2008) Molecular analysis of the spatio-temporal distribution of sulfate-reducing bacteria (SRB) in Camargue (France) hypersaline microbial mat. *Microb. Ecol.* **56**, 90–100.

Fourcans A., Sole A., Diestra E., Ranchou-Peyruse A., Esteve I., Caumette P. and Duran R. (2006) Vertical migration of phototrophic bacterial populations in a hypersaline microbial mat from Salins-de-Giraud (Camargue, France). *FEMS Microbiol. Ecol.* **57**, 367–377.

Frund C. and Cohen Y. (1992) Diurnal cycles of sulfate reduction under oxic conditions in cyanobacterial mats. *Appl. Environ. Microbiol.* **58**, 70–77.

Fry B., Cox J., Gest H. and Hayes J. M. (1986a) Discrimination between S-34 and S-32 during bacterial metabolism of inorganic sulfur-compounds. *J. Bacteriol.* **165**, 328–330.

Fry B., Gest H. and Hayes J. M. (1984) Isotope effects associated with the anaerobic oxidation of sulfide by the purple photosynthetic bacterium, Chromatium Vinosum. *FEMS Microbiol. Lett.* **22**, 283–287.

Fry B., Gest H. and Hayes J. M. (1985) Isotope effects associated with the anaerobic oxidation of sulfite and thiosulfate by the photosynthetic bacterium *Chromatium vinosum*. *FEMS Microbiol. Lett.* **27**, 227–232.

Fry B., Gest H. and Hayes J. M. (1986b) Sulfur isotope effects associated with protonation of HS^- and volatilization of H_2S. *Chem. Geol.* **58**, 253–258.

Fry B., Gest H. and Hayes J. M. (1988a) S-34/S-32 fractionation in sulfur cycles catalyzed by anaerobic bacteria. *Appl. Environ. Microbiol.* **54**, 250–256.

Fry B., Ruf W., Gest H. and Hayes J. M. (1988b) Sulfur isotope effects associated with oxidation of sulfide by O-2 in aqueous solution. *Chem. Geol.* **73**, 205–210.

Fukui M., Teske A., Aßmus B., Muyzer G. and Widdel F. (1999) Physiology, phylogenetic relationships, and ecology of filamentous sulfate-reducing bacteria (genus Desulfonema). *Arch. Microbiol.* **172**, 193–203.

Fuseler K. and Cypionka H. (1995) Elemental sulfur as an intermediate of sulfide oxidation with oxygen by *Desulfobulbus proprionicus*. *Arch. Microbiol.* **164**, 104–109.

Fuseler K., Krekeler D., Sydow U. and Cypionka H. (1996) A common pathway of sulfide oxidation by sulfate-reducing bacteria. *FEMS Microbiol. Lett.* **144**, 129–134.

Garrels R. M. and Lerman A. (1981). Phanerozoic cycles of sedimentary carbon and sulfur. *Proc. Natl. Acad. Sci. USA* **78**.

Gill B. C., Lyons T. W. and Saltzman M. R. (2007) Parallel, high-resolution carbon and sulfur isotope records of the evolving Paleozoic marine sulfur reservoir. *Palaeogeogr. Palaeocl.* **256**, 156–173.

Green S. J., Blackford C., Bucki P., Jahnke L. L. and Prufert-Bebout L. (2008) A salinity and sulfate manipulation of hypersaline microbial mats reveals stasis in the cyanobacterial community structure. *ISME J.* **2**, 457–470.

Habicht K. S. and Canfield D. E. (1996) Sulphur isotope fractionation in modern microbial mats and the evolution of the sulphur cycle. *Nature* **382**.

Habicht K. S. and Canfield D. E. (1997) Sulfur isotope fractionation during bacterial sulfate reduction in organic-rich sediments. *Geochim. Cosmochim. Acta* **61**, 5351–5361.

Habicht K. S., Canfield D. E. and Rethmeier J. (1998) Sulfur isotope fractionation during bacterial reduction and disproportionation of thiosulfate and sulfite. *Geochim. Cosmochim. Acta* **62**, 2585–2595.

Habicht K. S., Gade M., Thamdrup B., Berg P. and Canfield D. E. (2002) Calibration of sulfate levels in the Archean ocean. *Science* **298**, 2372–2374.

Halverson G. P. and Hurtgen M. T. (2007) Ediacaran growth of the marine sulfate reservoir. *Earth Planet. Sci. Lett.* **263**, 32–44.

Harrison A. G. and Thode H. G. (1958) Mechanisms of the bacterial reduction of sulfate from isotope fractionation studies. *Trans. Faraday Soc.* **54**, 84–92.

Hinck S., Neu T. R., Lavik G., Mussmann M., de Beer D. and Jonkers H. M. (2007) Physiological adaptation of a nitrate-storing *Beggiatoa* sp. to diel cycling in a phototrophic hypersaline mat. *Appl. Environ. Microbiol.* **73**, 7013–7022.

Hoehler T. M., Albert D. B., Alperin M. J., Bebout B. M., Martens C. S. and Des Marais D. J. (2002) Comparative ecology of H_2 cycling in sedimentary and phototrophic ecosystems. *Antonie van Leeuwenhoek* **81**, 575–585.

Hoehler T. M., Bebout B. M. and Des Marais D. J. (2001) The role of microbial mats in the production of reduced gases on the early Earth. *Nature* **412**, 324–327.

Hoek J., Reysenback A.-L., Habicht K. S. and Canfield D. E. (2006) Effect of hydrogen limitation and temperature on the

fractionation of sulfur isotopes by a deep-sea hydrothermal vent sulfate-reducing bacterium. *Geochim. Cosmochim. Acta* **70**, 5831–5841.

Holser W. T. (1977) Catastrophic chemical events in history of ocean. *Nature* **267**, 403–408.

Holser W. T. and Kaplan I. R. (1966) Isotope geochemistry of sedimentary sulfates. *Chem. Geol.* **1**, 93–135.

Holser W. T., Schidlowski M., Mackenzie F. T. and Maynard J. B. (1988) Geochemical cycles of carbon and sulfur. In *Chemical Cycles in the Evolution of the Earth* (eds. C. B. Gregor, R. M. Garrels, F. T. MacKenzie and J. B. Maynard). John Wiley & Sons, New York.

Hurtgen M. T., Arthur M. A. and Halverson G. P. (2005) Neoproterozoic sulfur isotopes, the evolution of microbial sulfur species, and the burial efficiency of sulfide as sedimentary pyrite. *Geology* **33**, 41–44.

Hurtgen M. T., Arthur M. A., Prave A. R., Amend J. P. e., Edwards K. J. e. and Lyons T. W. e. (2004) The sulfur isotope composition of carbonate-associated sulfate in Mesoproterozoic to Neoproterozoic carbonates from Death Valley, California. *Sulfur Biogeochem. Past Present* **379**, 177–194.

Hurtgen M. T., Pruss S. B. and Knoll A. H. (2009) Evaluating the relationship between the carbon and sulfur cycles in later Cambrian ocean: an example from the Port au Port Group, western Newfoundland, Canada. *Earth Planet. Sci. Lett.* **281**, 288–297.

Jahnke L. L., Orphan V. J., Embaye T., Turk K. A., Kubo M., Summons R. E. and Des Marais D. J. (2008) Lipid biomarker and phylogenetic analyses to reveal archaeal biodiversity and distribution in a hypersaline microbial mat and underlying sediment. *Geobiology* **6**, 394–410.

Johnston D. T., Farquhar J., Wing B. A., Kaufman A. J., Canfield D. E. and Habicht K. S. (2005) Multiple sulfur isotope fractionations in biological systems: a case study with sulfate reducers and sulfur disproportionators. *Am. J. Sci.* **305**, 645–660.

Jorgensen B. B. (1990) A thiosulfate shunt in the sulfur cycle of marine sediments. *Science* **249**, 152–154.

Jorgensen B. B. (1994) Sulfate reduction and thiosulfate transformations in a cyanobacterial mat during a diel oxygen cycle. *FEMS Microbiol. Ecol.* **13**, 303–312.

Jorgensen B. B., Cohen Y. and Revsbech N. P. (1986) Transition from anoxygenic to oxygenic photosynthesis in a *Microcoleus chthonoplastes* cyanobacterial mat. *Appl. Environ. Microbiol.* **51**, 408–417.

Jorgensen B. B. and Des Marais D. J. (1986) Competition for sulfide among colorless and purple sulfur bacteria in cyanobacterial mats. *FEMS Microbiol. Ecol.* **38**, 179–196.

Jorgensen B. B. and Des Marais D. J. (1990) The diffusive boundary-layer of sediments – oxygen microgradients over a microbial mat. *Limnol. Oceanogr.* **35**, 1343–1355.

Kampschulte A. and Strauss H. (2004) The sulfur isotopic evolution of Phanerozoic seawater based on the analysis of structurally substituted sulfate in carbonates. *Chem. Geol.* **204**, 255–286.

Kaplan I. R. and Rittenberg S. C. (1964) Microbiological fractionation of sulphur isotopes. *J. Gen. Microbiol.* **34**, 195–212.

Kemp A. L. W. and Thode H. G. (1968) Mechanism of bacterial reduction of sulphate and of sulphite from isotope fractionation studies. *Geochim. Cosmochim. Acta* **32**, 71

Krekeler D., Sigalevich P., Teske A., Cypionka H. and Cohen Y. (1997) A sulfate-reducing bacterium from the oxic layer of a microbial mat from Solar Lake (Sinai), *Desulfovibrio oxyclinae* sp. nov. *Arch. Microbiol.* **167**, 369–375.

Krekeler D., Teske A. and Cypionka H. (1998) Strategies of sulfate-reducing bacteria to escape oxygen stress in a cyanobacterial mat. *FEMS Microbiol. Ecol.* **25**, 89–96.

Kunin V., Raes J., Harris J. K., Spear J. R., Walker J. J., Ivanova N., von Mering C., Bebout B. M., Pace N. R., Bork P. and Hugenholtz P. (2008) Millimeter-scale genetic gradients and community-level molecular convergence in a hypersaline microbial mat. *Mol. Syst. Biol.* **4**, 198.

Ley R. E., Harris J. K., Wilcox J., Spear J. R., Miller S. R., Bebout B. M., Maresca J. A., Bryant D. A., Sogin M. L. and Pace N. R. (2006) Unexpected diversity and complexity of the Guerrero Negro hypersaline microbial mat. *Appl. Environ. Microbiol.* **72**, 3685–3695.

Manz W., Eisernbrecher M., Neu T. R. and Szewzyk U. (1998) Abundance and spatial organization of Gram-negative sulfate-reducing bacteria in activated sludge investigated by in situ probing with specific 16S rRNA targeted oligonucleotides. *FEMS Microbiol. Ecol.* **25**, 43–61.

Minz D., Fishbain S., Green S. J., Muyzer G., Cohen Y., Rittmann B. E. and Stahl D. A. (1999a) Unexpected population distribution in a microbial mat community: sulfate-reducing bacteria localized to the highly oxic chemocline in contrast to a eukaryotic preference for anoxia. *Appl. Environ. Microbiol.* **65**, 4659–4665.

Minz D., Flax J. L., Green S. J., Muyzer G., Cohen Y., Wagner M., Rittmann B. E. and Stahl D. A. (1999b) Diversity of sulfate-reducing bacteria in oxic and anoxic regions of a microbial mat characterized by comparative analysis of dissimilatory sulfite reductase genes. *Appl. Environ. Microbiol.* **65**, 4666–4671.

Orphan V. J., Jahnke L. L., Embaye T., Turk K. A., Pernthaler A., Summons R. E. and Des Marais D. J. (2008) Characterization and spatial distribution of methanogens and methanogenic biosignatures in hypersaline microbial mats of Baja California. *Geobiology* **6**, 376–393.

Pernthaler A., Pernthaler J. and Amann R. (2002) Fluorescence in situ hybridization and catalyzed reporter deposition for the identification of marine bacteria. *Appl. Environ. Microbiol.* **68**, 3094–3101.

Porter D., Roychoudhury A. N. and Cowan D. (2007) Dissimilatory sulfate reduction in hypersaline coastal pans: activity across a salinity gradient. *Geochim. Cosmochim. Acta* **71**, 5102–5116.

Rees C. E. (1973) Steady-state model for sulfur isotope fractionation in bacterial reduction processes. *Geochim. Cosmochim. Acta* **37**, 1141–1162.

Revsbech N. P., Jorgensen B. B., Blackburn T. H. and Cohen Y. (1983) Microelectrode studies of the photosynthesis and O_2, H_2S, and pH profiles of a microbial mat. *Limnol. Oceanogr.* **28**, 1062–1074.

Risatti J. B., Capman W. C. and Stahl D. A. (1994) Community structure of a microbial mat: the phylogenetic dimension. *Proc. Natl. Acad. Sci.* **91**, 10173–10177.

Robertson C. E., Spear J. R., Harris J. K. and Pace N. R. (2009) Diversity and stratification of archaea in a hypersaline microbial mat. *Appl. Environ. Microbiol.* **75**.

Ross G. M., Bloch J. D. and Krouse H. R. (1995) Neoproterozoic strata of the southern Canadian Cordillera and the isotopic evolution of seawater sulfate. *Precambrian Res.* **73**, 71–99.

Sagemann J., Jorgensen B. B. and Greeff O. (1998) Temperature dependence and rates of sulfate reduction in cold sediments of Svalbard, Arctic Ocean. *Geomicrobiol. J.* **15**, 85–100.

Sigalevich P., Baev M. V., Teske A. and Cohen Y. (2000) Sulfate reduction and possible aerobic metabolism of the sulfate-reducing bacterium *Desulfovibrio oxyclinae* in a chemostat coculture with *Marinobacter* sp strain MB under exposure to increasing oxygen concentrations. *Appl. Environ. Microbiol.* **66**, 5005–5012.

Spear J. R., Ley R. E., Berger A. B. and Pace N. R. (2003) Complexity in natural microbial ecosystems: the Guerrero Negro experience. *Biol. Bull.* **204**, 168–173.

Teske A., Ramsing N. B., Habicht K., Fukui M., Kuver J., Jorgensen B. B. and Cohen Y. (1998) Sulfate-reducing bacteria and their activities in cyanobacterial mats of Solar Lake (Sinai, Egypt). *Appl. Environ. Microbiol.* **64**, 2943–2951.

Thode H. D. and Monster J. (1965) *Sulfur-Isotope Geochemistry of Petroleum, Evaporites, and Ancient Seas, Fluids in Subsurfaces Environments, Memoir 4*. American Association of Petroleum Geologists, Tulsa, OK.

Thode H. G. (1980) Sulfur isotope ratios in late and early Precambrian sediments and their implications regarding early environments and early life. *Orig. Life Evol. Biosph.* **10**, 127–136.

Visscher P. T., Baumgartner L. K., Buckley D. H., Rogers D. R., Hogan M. E., Raleigh C. D., Turk K. A. and Des Marais D. J. (2003) Dimethyl sulphide and methanethiol formation in microbial mats: potential pathways for biogenic signatures. *Environ. Microbiol.* **5**, 296–308.

Visscher P. T., Prins R. A. and Vangemerden H. (1992) Rates of sulfate reduction and thiosulfate consumption in a marine microbial mat. *FEMS Microbiol. Ecol.* **86**, 283–293.

Visscher P. T., Reid R. P. and Bebout B. M. (2000) Microscale observations of sulfate reduction: correlation of microbial activity with lithified micritic laminae in modern marine stromatolites. *Geology* **28**, 919–922.

Watanabe Y., Farquhar J. and Ohmoto H. (2009) Anomalous fractionations of sulfur isotopes during thermochemical sulfate reduction. *Science* **324**, 370–373.

Werne J. P., Lyons T. W., Hollander D. J., Formolo M. J. and Damste J. S. S. (2003) Reduced sulfur in euxinic sediments of the Cariaco Basin: sulfur isotope constraints on organic sulfur formation. *Chem. Geol.* **195**, 159–179.

Wieland A., de Beer D., Damgaard L. R., Kuehl M., van Dusschoten D. and Van As H. (2001) Fine-scale measurement of diffusivity in a microbial mat with nuclear magnetic resonance imaging. *Limnol. Oceanogr.* **46**, 248–259.

Wieringa E. B. A., Overmann J. and Cypionka H. (2000) Detection of abundant sulphate-reducing bacteria in marine oxic sediment layers by a combined cultivation and molecular approach. *Environ. Microbiol.* **2**, 417–427.

Wortmann U. G., Bernasconi S. M. and Boettcher M. E. (2001) Hypersulfidic deep biosphere indicates extreme sulfur isotope fractionation during single step microbial sulfate reduction. *Geology* **29**, 647–650.

Associate editor: Juske Horita